Electronic Supplementary Material (ESI) for Dalton Transactions.

Supporting Information

Bidentate Boron Lewis Acids: Synthesis by Tin Boron Exchange Reaction and Host-Guest Complex Formation

J. Louis Beckmann, Beate Neumann, Hans-Georg Stammler, Jan-Hendrik Lamm and Norbert W. Mitzel*

*Corresponding Author.

Chair of Inorganic and Structural Chemistry, Center for Molecular Materials CM_2
Faculty of Chemistry, University of Bielefeld
Universitätsstraße 25, 33615 Bielefeld (Germany)
E-mail: mitzel@uni-bielefeld.de

Table of Contents

Experimental Procedures

General considerations

All reactions were performed in the absence of water and air using conventional Schlenk techniques with nitrogen as inert gas or in a glove box with argon as inert gas. For handling volatile compounds and gases, conventional high vacuum techniques were used. *n*-Pentane, *n*-hexane and diethyl ether were dried over lithium aluminum hydride. Dichloromethane and chloroform were dried over calcium hydride or with molecular sieve. Benzene and THF were dried over Na/K alloy. All solvents were degassed prior to use and stored with molecular sieve.

1,8-Bis[(trimethylstannyl)ethynyl]anthracene (**1**)[1], 2-chloro-2-boraindane diethyl etherate (**2a**)[2], chlorodiethylborane (**2c**)[3], trimethylborane,[4] chlorobis(pentafluorophenyl)borane (**2d**)[5] and bis(pentafluorophenyl)borane[5,6] were prepared according to literature.

NMR spectra were recorded on a Avance III 500 HD and Avance NEO 600 spectrometer at ambient temperature, unless otherwise stated. Chemical shifts were referenced to the residual proton or carbon signal of the solvent ($CDCl_3$: ^{1}H: 7.26 ppm, ^{13}C: 77.2 ppm; C_6D_6: ^{1}H: 7.16 ppm, ^{13}C: 128.1 ppm; DMSO-d_6: ^{1}H: 2.50 ppm, ^{13}C: 39.5 ppm) or externally (^{11}B: $BF_3{\cdot}OEt_2$, ^{19}F: $CFCl_3$). Elemental analyses were carried out using an EURO EA Elemental Analyzer. SC-XRD was performed on a Rigaku Supernova diffractometer using Cu-Kα or Mo-Kα radiation.

The numbering scheme for NMR spectroscopic assignments of the anthracenes (Scheme S1) is based on IUPAC guidelines.

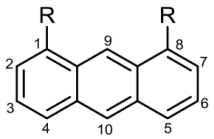

Scheme S1. Numbering scheme for NMR spectroscopic assignments.

Syntheses

1,8-Bis[(2-boraindan-2-yl)ethynyl]anthracene (3a): A suspension of 2-chloro-2-boraindane diethyl etherate (**2a**, 1.20 g, 5.34 mmol) in *n*-hexane (15 mL) was added to 1,8-bis[(trimethylstannyl)ethynyl]anthracene (**1**, 1.25 g, 2.26 mmol) in *n*-hexane (20 mL) at −10 °C. The reaction mixture was stirred for 5 h at 0 °C, allowed to reach ambient temperature and was stirred for an additional hour. The suspension was centrifuged (2000 rpm, 40 minutes) to precipitate the crude product as a yellow solid. The supernatant solution was removed, the precipitate resuspended in benzene (15 mL), stirred for additional 10 minutes and centrifuged again. The supernatant solution was removed, all volatile compounds were removed under reduced pressure and 1,8-Bis[(2-boraindan-2-yl)ethynyl]anthracene (**3a**, 0.92 g, 2.02 mmol, 89 %) was obtained as a yellow solid. – ^{1}H NMR (500 MHz, $CDCl_3$): δ [ppm] = 9.48 (s, 1H, H9), 8.53 (s, 1H, H10), 8.12 (d, $^3J_{H,H}$ = 8.5 Hz, 2H, H4/H5), 7.92 (d, $^3J_{H,H}$ = 6.9 Hz, 2H, H2/H7), 7.54 (dd, $^3J_{H,H}$ = 8.5 Hz, 6.9 Hz, 2H, H3/H6), 7.17 (m, 8H, H^{Ph}), 2.95 (s, 8H, CH_2). – ^{13}C{^{1}H} NMR (126 MHz, $CDCl_3$): δ [ppm] = 145.0 (s, $C^{Ph\text{-}i}$), 132.9 (s, C2/C7), 131.6 (s, C^q), 131.3 (s, C^q), 131.0 (s, C4/C5), 128.2 (s, C10), 127.3 (s, C^{Ph}), 126.2 (s, C^{Ph}), 125.4 (s, C3/C6), 124.1 (s, C9), 122.9 (s, **C**≡C–B), 120.8 (s, C^q), 36.9 (s, CH_2). – ^{11}B NMR (160 MHz, $CDCl_3$): δ [ppm] = 79.2 (s). – Elemental analysis calcd (%) for $C_{34}H_{24}B_2$ (M_r = 454.2): C 89.91, H 5.33; found: C 89.90, H 5.36.

Chlorodimethylborane (Me_2BCl, 2b): This protocol is a derived version of the synthesis of chlorodiethylborane (Et_2BCl, **2c**) described by Breher et al.[3]

To an ampoule filled with $NaBH_4$ (15 mg), dichloromethane (10 mL) was added. Trimethylborane (20.0 mmol) and boron trichloride (10.0 mmol) were added by condensation using a high vacuum line. The reaction mixture was stirred for 5 d at

ambient temperature and additional 5 d at 40°C. Distillation of the reaction mixture yields chlorodimethylborane (**2b**, 26.4 mmol, 88 %). – ^{1}H NMR (500 MHz, $CDCl_3$): δ [ppm] = 1.02 (s, 6H, CH_3). – $^{13}C\{^{1}H\}$ NMR (126 MHz, $CDCl_3$): δ [ppm] = 15.4 (s, CH_3). – ^{11}B NMR (160 MHz, $CDCl_3$): δ [ppm] = 77.0.

1,8-Bis[(dimethylboranyl)ethynyl]anthracene (3b): To a suspension of 1,8-bis[(trimethylstannyl)ethynyl]anthracene (**1**, 0.40 g, 0.72 mmol) in *n*-hexane (12 mL), chlorodimethylborane (**2b**, 2.5 mmol) was added by condensation using a high vacuum line. The reaction mixture was stirred for 15 min and allowed to reach room temperature. Longer reaction times or temperatures above ambient temperature should be avoided, as these will strongly promote side reactions. All volatile compounds were removed under reduced pressure and 1,8-bis[(dimethylboranyl)ethynyl]anthracene (**3b**, 0.22 g, 0.72 mmol, quant.) was obtained as a yellow solid. – ^{1}H NMR (500 MHz, $CDCl_3$): δ [ppm] = 9.41 (s, 1H, H9), 8.46 (s, 1H, H10), 8.05 (d, $^{3}J_{H,H}$ = 8.6 Hz, 2H, H4/H5), 7.81 (d, $^{3}J_{H,H}$ = 6.9 Hz, 2H, H2/H7), 7.48 (dd, $^{3}J_{H,H}$ = 8.6 Hz, 6.9 Hz, 2H, H3/H6), 1.08 (s, 12H, CH_3). – $^{13}C\{^{1}H\}$ NMR (126 MHz, $CDCl_3$): δ [ppm] = 132.0 (s, C2/C7), 131.6 (s, C^q), 131.3 (s, C^q), 130.2 (s, C4/C5), 127.8 (s, C10), 125.3 (s, C3/C6), 124.2 (s, C9), 121.3 (s, C^q), 116.3 (s, **C**≡C–B), 105.7 (s, C≡**C**–B), 15.8 (s, CH_3). – ^{11}B NMR (160 MHz, $CDCl_3$): δ [ppm] = 72.1 (s). – Elemental analysis calcd (%) for $C_{22}H_{20}B_2$ (M_r = 306.0): C 86.35, H 6.59; found: C 85.32, H 6.09.

1,8-Bis[(diethylboranyl)ethynyl]anthracene (3c): To a suspension of 1,8-bis[(trimethylstannyl)ethynyl]anthracene (**1**, 1.00 g, 1.81 mmol) in *n*-hexane (16 mL), a solution of chlorodiethylborane (**2c**, 5.5 mmol) in dichloromethane was added with a syringe at 0 °C. The reaction mixture was stirred for 1 h at 0 °C, allowed to reach ambient temperature and was stirred for additional 0.5 h. All volatile compounds were removed under reduced pressure and 1,8-bis[(diethylboranyl)ethynyl]anthracene (**3c**, 0.66 g, 1.81 mmol, quant.) was obtained as a yellow solid. – ^{1}H NMR (600 MHz, $CDCl_3$): δ [ppm] = 9.42 (s, 1H, H9), 8.45 (s, 1H, H10), 8.03 (d, $^{3}J_{H,H}$ = 8.5 Hz, 2H, H4/H5), 7.81 (d, $^{3}J_{H,H}$ = 6.9 Hz, 2H, H2/H7), 7.47 (dd, $^{3}J_{H,H}$ = 8.5 Hz, 6.9 Hz, 2H, H3/H6), 1.43 (q, $^{3}J_{H,H}$ = 7.6 Hz, 8H, CH_2), 1.20 (t, $^{3}J_{H,H}$ = 7.5 Hz, 12H, CH_3). – $^{13}C\{^{1}H\}$ NMR (150 MHz, $CDCl_3$): δ [ppm] = 131.9 (s, C2/C7), 131.6 (s, C^q), 131.3 (s, C^q), 130.0 (s, C4/C5), 127.8 (s, C10), 125.3 (s, C3/C6), 124.3 (s, C9), 121.5 (s, C^q), 118.6 (s, **C**≡C–B), 103.9 (s, C≡**C**–B), 21.7 (s, CH_2), 9.6 (s, CH_3). – ^{11}B NMR (160 MHz, $CDCl_3$): δ [ppm] = 74.6 (s). – Elemental analysis calcd (%) for $C_{26}H_{28}B_2$ (M_r = 362.1): C 86.24, H 7.79; found: C 85.56, H 7.66.

1,8-Bis[{bis(pentafluorophenyl)boranyl}ethynyl]anthracene (3d): To a suspension of 1,8-bis[(trimethylstannyl)ethynyl]-anthracene (**1**, 1.10 g, 2.00 mmol) in *n*-hexane (15 mL), a solution of chlorobis(pentafluorophenyl)borane (**2d**, 1.90 g, 5.00 mmol) in *n*-hexane (20 mL) was slowly added at −80 °C with a syringe. The reaction mixture was stirred for 3 h at 0 °C, allowed to reach ambient temperature and was stirred for another hour. The suspension was centrifuged (2000 rpm, 20 minutes) to precipitate the crude product as a red solid, from which the supernatant solution was removed. To purify the product, the precipitate was resuspended in *n*-hexane (10 mL) and stirred for 10 min. The suspension was centrifuged and the supernatant solution was removed. This washing procedure was repeated once more with *n*-hexane (10 mL) and then with benzene (10 mL). All volatiles were then removed under reduced pressure and 1,8-bis[{bis(pentafluorophenyl)boranyl}ethynyl]anthracene (**3d**, 1.60 g, 1.75 mmol, 88 %) was obtained as a red solid. NMR spectroscopic data are provided in C_6D_6 and DMSO-d_6 as solvent, since the solubility in $CDCl_3$ is very limited. No ^{11}B NMR signal was observed due to strong broadening. – ^{1}H NMR (500 MHz, C_6D_6): δ [ppm] = 9.91 (s, 1H, H9), 7.92 (s, 1H, H10), 7.83 (d, $^{3}J_{H,H}$ = 7.0 Hz, 2H, H2/H7), 7.62 (d, $^{3}J_{H,H}$ = 8.5 Hz, 2H, H4/H5), 6.96 (dd, $^{3}J_{H,H}$ = 8.5 Hz, 7.0 Hz, 2H, H3/H6). – ^{19}F NMR (470 MHz, C_6D_6): δ [ppm] = −127.6 (m, $F^{Ph\text{-}o}$), −145.0 (m, $F^{Ph\text{-}p}$), −160.9 (m, $F^{Ph\text{-}m}$). – ^{1}H NMR (500 MHz, DMSO-d_6): δ [ppm] = 9.32 (s, 1H, H9), 8.70 (s, 1H, H10), 8.11 (d, $^{3}J_{H,H}$ = 8.6 Hz, 2H, H4/H5), 7.78 (d, $^{3}J_{H,H}$ = 6.9 Hz, 2H, H2/H7), 7.54 (dd, $^{3}J_{H,H}$ = 8.5 Hz, 6.9 Hz, 2H, H3/H6). – $^{13}C\{^{1}H\}$ NMR (126 MHz, DMSO-d_6): δ [ppm] = 147.1 (d, $^{1}J_{C,F}$ = 242 Hz, C^{Ph}), 138.7 (d, $^{1}J_{C,F}$ = 247 Hz, C^{Ph}), 136.1 (d, $^{1}J_{C,F}$ = 247 Hz, C^{Ph}), 131.7 (s, C2/C7), 131.2 (s, C^q), 130.5 (s, C^q), 128.4 (s, C4/C5), 128.28, 128.0 (s, C10), 125.4 (s, C3/C6), 122.8 (s, C9), 122.4 (s, C^q), 119.8 (m, $C^{Ph\text{-}i}$), 106.6 (s, C≡**C**–B), 98.1 (s, **C**≡C–B). – ^{19}F NMR (470 MHz, DMSO-d_6): δ [ppm] = −133.0 (m, $F^{Ph\text{-}o}$), −159.4 (m, $F^{Ph\text{-}p}$), −164.8 (m, $F^{Ph\text{-}m}$). – Elemental analysis calcd (%) for $C_{42}H_8B_2F_{20}$ (M_r = 914.1): C 55.19, H 0.88; found: C 54.80, H 0.83.

1,8-Bis[{2,2-bis(pentafluorophenyl)boranyl}vinyl]anthracene (4d): To a suspension of 1,8-bis[{bis(pentafluorophenyl)-boranyl}ethynyl]anthracene (**3d**, 180 mg, 197 µmol) in benzene (6 mL), bis(pentafluorophenyl)borane (170 mg, 0.49 mmol) was added at ambient temperature. The reaction mixture was stirred for 1 d, the product was allowed to precipitate, and the supernatant solution was removed. After recrystallization from benzene and removal of all volatile compounds under reduced pressure, 1,8-bis[{1,2-bis(pentafluorophenyl)boranyl}vinyl]anthracene (**4d**, 230 mg, 143 µmol, 73 %) was obtained as an orange solid. No ^{11}B NMR signal was observed due to strong broadening. – ^{1}H NMR (500 MHz, $CDCl_3$): δ [ppm] = 8.88 (s, 2H, C=CH), 8.31 (s, 1H, H10), 7.93 (d, $^{3}J_{H,H}$ = 8.6 Hz, 2H, H4/H5), 7.84 (s, 1H, H9), 7.36 (dd, $^{3}J_{H,H}$ = 8.6 Hz, 6.7 Hz, 2H, H3/H6), 7.21 (d, $^{3}J_{H,H}$ = 6.7 Hz, 2H, H2/H7). – ^{13}C{^{1}H} NMR (126 MHz, $CDCl_3$): δ [ppm] = 172.0 (s, C=**C**H), 155.0 (s, **C**=CH), 148.0 (d, $^{1}J_{C,F}$ = 250 Hz, C^{Ph}), 146.9 (d, $^{1}J_{C,F}$ = 247 Hz, C^{Ph}), 143.5 (d, $^{1}J_{C,F}$ = 266 Hz, C^{Ph}), 139.4 (s, C^{q}), 137.6 (d, $^{1}J_{C,F}$ = 255 Hz, C^{Ph}), 137.0 (d, $^{1}J_{C,F}$ = 256 Hz, C^{Ph}), 132.4 (s, C4/C5), 131.1 (s, C^{q}), 129.5 (s, C2/C7), 128.5 (s, C10), 128.1 (s, C^{q}), 125.6 (s, C3/C6), 121.8 (s, C9), 113.8 (m, $C^{Ph\text{-}i}$). – ^{19}F NMR (470 MHz, $CDCl_3$): δ [ppm] = −127.0 (m, $F^{Ph\text{-}o}$), −129.1 (m, $F^{Ph\text{-}o}$), −145.2 (m, $F^{Ph\text{-}p}$), −146.8 (m, $F^{Ph\text{-}p}$), −160.5 (m, $F^{Ph\text{-}m}$), −161.2 (m, $F^{Ph\text{-}m}$). – Elemental analysis calcd (%) for $C_{66}H_{10}B_4F_{40}$ (M_r = 1606.0): C 49.36, H 0.63; found: C 48.97, H 0.60.

General procedure for the preparation of the adducts of 3a, 3c and 3d with pyridine, pyrimidine and TMEDA

The respective 1:1- or 1:2-adducts were prepared in quantitative yield by adding one or two equivalents of guest (depending on the respective adduct) to a solution of host compound **3a**, **3c** or **3d**. When the components were mixed, a color change from intense yellow or red towards pale yellow was observed. The adducts were characterized by various NMR spectroscopic experiments (^{1}H NMR, ^{19}F NMR, ^{11}B NMR, ^{13}C{^{1}H} NMR, ^{1}H,^{1}H COSY NMR, ^{1}H,^{13}C HMBC and HMQC NMR); the analytical data for these adducts are provided further below. Adducts of **3d** were measured in C_6D_6 instead of $CDCl_3$ to maintain comparability (the free host **3d** is insoluble in $CDCl_3$ but soluble in C_6D_6). No NMR data are given for [**3a**·TMEDA] and [**3d**·TMEDA] because these adducts precipitate quantitatively seconds after TMEDA addition, leaving only traces of the substance in the supernatant solution. In the case of [**3c**·TMEDA], the majority precipitated, and only small amounts remained soluble, so this supernatant solution was analyzed by NMR spectroscopy. By cooling these solutions or reducing the amount of solvent, precipitates were also obtained for the more soluble adducts. In case of [**3a**·2 Py], [**3c**·2 Py], [**3d**·2 Py], [**3a**·TMEDA], [**3c**·TMEDA], [**3c**·Pym] and [**3d**·Pym], these precipitates were crystalline and provided single crystals suitable for SC X-ray diffraction (see further below for details of the SC XRD measurements). The precipitates formed were dried under reduced pressure and examined by elemental analyses. No elemental analysis of [**3a**·Pym] was performed as no precipitate could be obtained at all and the NMR spectra show the presence of different species in solution.

Analytical data of the adducts

3a·2 Py – ^{1}H NMR (500 MHz, $CDCl_3$): δ [ppm] = 9.80 (s, 1H, H9), 8.89 (m, 4H, $H^{Py\text{-}o}$), 8.41 (s, 1H, H10), 7.92 (d, $^{3}J_{H,H}$ = 8.5 Hz, 2H, H4/H5), 7.77 – 7.71 (m, 4H, $H^{Py\text{-}p}$ and H2/H7), 7.41 (dd, $^{3}J_{H,H}$ = 8.5 Hz, 6.9 Hz, 2H, H3/H6), 7.34 (m, 4H, $H^{Py\text{-}m}$), 7.11 – 7.06 (m, 4H, H^{Ph}), 7.02 – 6.98 (m, 4H, H^{Ph}), 2.48 (d, $^{2}J_{H,H}$ = 17.6 Hz, 4H, C**H**^{a}H^{b}), 1.95 (d, $^{2}J_{H,H}$ = 17.6 Hz, 4H, CH^{a}**H**^{b}). – ^{13}C{^{1}H} NMR (126 MHz, $CDCl_3$): δ [ppm] = 148.7 (s, $C^{Ph\text{-}i}$), 144.9 (s, $C^{Py\text{-}o}$), 139.8 (s, $C^{Py\text{-}p}$), 131.9 (s, C^{q}), 131.7 (s, C^{q}), 130.3 (s, C2/C7), 127.5 (s, C4/C5), 127.3 (s, C^{Ph}), 127.2 (s, C10), 125.5 (s, $C^{Py\text{-}m}$), 125.2 (s, C3/C6), 124.9 (s, C9), 124.9 (s, C^{Ph}), 124.2 (s, C^{q}), 112.9 (s, C≡**C**–B), 97.6 (s, **C**≡C–B), 34.1 (s, CH_2). – ^{11}B NMR (160 MHz, $CDCl_3$): δ [ppm] = 0.7 (s). – Elemental analysis calcd (%) for $C_{44}H_{34}B_2N_2$ (M_r = 612.4): C 86.30, H 5.60, N 4.57; found: C 85.99, H 5.63, N 4.64.

3a·Pym – ^{1}H NMR (600 MHz, $CDCl_3$): δ [ppm] = 11.15 (s, 1H, N(CH)N), 9.73 – 9.45 (br. m, 1H, H9), 8.94 – 8.45 (br. m, 2H, N(C**H**)C), 8.30 (s, 1H, H10), 7.83 (d, $^{3}J_{H,H}$ = 8.6 Hz, 2H, H4/H5), 7.59 (d, $^{3}J_{H,H}$ = 6.8 Hz, 2H, H2/H7), 7.32 (dd, $^{3}J_{H,H}$ = 8.6 Hz, 6.8 Hz, 2H, H3/H6), 7.23 – 7.15 (m, 1H, NCH(C**H**)), 7.11 – 6.88 (br. m, 8H, H^{Ph}), 3.00 – 1.62 (br. m, 8H, CH_2). – ^{13}C{^{1}H} NMR (150 MHz, $CDCl_3$): δ [ppm] = 154.9 (s, NCN), 153.5 (s, N**C**C), 146.7 (s, $C^{Ph\text{-}i}$), 131.5 (s, C^{q}), 131.2 (s, C^{q}), 128.6 (s, C2/C7), 127.7 (s, C4/C5), 127.5 (s, C^{Ph}), 127.0 (s, C10), 125.9 (s, C^{Ph}), 125.5 (s, C3/C6), 125.1 (s, C9), 123.2 (s, C^{q}), 122.8 (s, NC**C**), 108.7 (s, C≡**C**–B), 99.3 (s, **C**≡C–B), 34.4 (s, CH_2). – ^{11}B NMR (160 MHz, $CDCl_3$): δ [ppm] = 0.7 (s).

3a·TMEDA – Elemental analysis calcd (%) for $C_{40.2}H_{40.2}B_2N_2Cl_{0.6}$ (**3a**·TMEDA·0.2 $CHCl_3$; M_r = 594.3): C 81.25, H 6.82, N 4.71; found: C 81.28, H 6.88, N 4.76.

3c·2 Py – ^{1}H NMR (500 MHz, $CDCl_3$): δ [ppm] = 9.72 (s, 1H, H9), 8.98 (m, 4H, $H^{Py\text{-}o}$), 8.40 (s, 1H, H10), 7.89 (d, $^3J_{H,H}$ = 8.5 Hz, 2H, H4/H5), 7.85 (m, 2H, $H^{Py\text{-}p}$), 7.76 (d, $^3J_{H,H}$ = 6.9 Hz, 2H, H2/H7), 7.51 (m, 4H, $H^{Py\text{-}m}$), 7.40 (dd, $^3J_{H,H}$ = 8.5 Hz, 6.9 Hz, 2H, H3/H6), 0.73 (t, $^3J_{H,H}$ = 7.4 Hz, 12H, CH_3), 0.64 (dq, $^2J_{H,H}$ = 15.3 Hz, $^3J_{H,H}$ = 7.7 Hz, 4H, C**H**^{a}H^b), 0.50 (dq, $^2J_{H,H}$ = 14.8 Hz, $^3J_{H,H}$ = 7.5 Hz, 4H, CH^a**H**^{b}). – ^{13}C{^{1}H} NMR (126 MHz, $CDCl_3$): δ [ppm] = 145.7 (s, $C^{Py\text{-}o}$), 139.4 (s, $C^{Py\text{-}p}$), 131.9 (s, C^q), 131.8 (s, C^q), 130.9 (s, C2/C7), 127.2 (s, C4/C5), 127.2 (s, C10), 125.2 (s, $C^{Py\text{-}m}$), 125.2 (s, C3/C6), 124.9 (s, C9), 124.8 (s, C^q), 114.2 (s, C≡**C**–B), 97.9 (s, **C**≡C–B), 18.1 (s, CH_2), 10.8 (s, CH_3). – ^{11}B NMR (160 MHz, $CDCl_3$): δ [ppm] = 0.7 (s). – Elemental analysis calcd (%) for $C_{36}H_{38}B_2N_2$ (M_r = 520.3): C 83.10, H 7.36, N 5.38; found: C 83.53, H 7.56, N 5.31.

3c·Pym – ^{1}H NMR (500 MHz, $CDCl_3$): δ [ppm] = 11.01 (br. m, 1H, N(CH)N), 9.78 (s, 1H, H9), 8.91 (br. m, 2H, N(C**H**)C), 8.40 (s, 1H, H10), 7.92 (d, $^3J_{H,H}$ = 8.5 Hz, 2H, H4/H5), 7.77 (m, 1H, NCH(C**H**)), 7.70 (d, $^3J_{H,H}$ = 6.9 Hz, 2H, H2/H7), 7.43 (dd, $^3J_{H,H}$ = 8.5 Hz, 6.9 Hz, 2H, H3/H6), 0.83 (t, $^3J_{H,H}$ = 7.3 Hz, 12H, CH_3), 0.73 (q, $^3J_{H,H}$ = 7.1 Hz, 8H, CH_2). – ^{13}C{^{1}H} NMR (126 MHz, $CDCl_3$): δ [ppm] = 155.6 (s, N**C**C), 154.4 (s, NCN), 131.5 (s, C^q), 131.2 (s, C^q), 128.4 (s, C2/C7), 127.3 (s, C4/C5), 126.7 (s, C10), 125.5 (s, C3/C6), 125.3 (s, C9), 123.8 (s, C^q), 122.4 (s, NC**C**), 109.9 (s, C≡**C**–B), 99.1 (s, **C**≡C–B), 18.5 (s, CH_2), 10.5 (s, CH_3). – ^{11}B NMR (160 MHz, $CDCl_3$): δ [ppm] = 1.8 (s). – Elemental analysis calcd (%) for $C_{30}H_{32}B_2N_2$ (M_r = 442.2): C 81.48, H 7.29, N 6.33; found: C 81.42, H 7.33, N 6.30.

3c·TMEDA – ^{1}H NMR (500 MHz, $CDCl_3$): δ [ppm] = 9.45 (s, 1H, H9), 8.36 (s, 1H, H10), 7.86 (d, $^3J_{H,H}$ = 8.5 Hz, 2H, H4/H5), 7.67 (d, $^3J_{H,H}$ = 6.9 Hz, 2H, H2/H7), 7.37 (t, 7.8 Hz, 2H, H3/H6), 3.79 – 3.40 (br. m, 4H, C_2H_4), 2.95 – 2.22 (br. m, 12H, NCH_3), 1.06 (t, $^3J_{H,H}$ = 7.5 Hz, 12H, CH_3), 0.57 (q, $^3J_{H,H}$ = 7.8 Hz, 8H, CH_2). – ^{13}C{^{1}H} NMR (126 MHz, $CDCl_3$): δ [ppm] = 131.7 (s, C^q), 131.7 (s, C^q), 130.0 (s, C2/C7), 127.2 (s, C10), 127.1 (s, C4/C5), 125.3 (s, C3/C6), 124.3 (s, C9), 112.7 (s, C≡**C**–B), 98.6 (s, **C**≡C–B), 55.6 (s, C_2H_4), 46.3 (s, NCH_3), 13.2 (s, CH_2), 12.0 (s, CH_3). – ^{11}B NMR (160 MHz, $CDCl_3$): δ [ppm] = 1.6 (s). – Elemental analysis calcd (%) for $C_{32}H_{44}B_2N_2$ (M_r = 478.3): C 80.35, H 9.27, N 5.86; found: C 79.91, H 9.05, N 5.53.

3d·2 Py – ^{1}H NMR (500 MHz, C_6D_6): δ [ppm] = 10.00 (s, 1H, H9), 8.79 (m, 4H, $H^{Py\text{-}o}$), 8.07 (s, 1H, H10), 7.86 (d, $^3J_{H,H}$ = 6.9 Hz, 2H, H2/H7), 7.62 (d, $^3J_{H,H}$ = 8.5 Hz, 2H, H4/H5), 7.07 (dd, $^3J_{H,H}$ = 8.5 Hz, 6.9 Hz, 2H, H3/H6), 6.83 (m, 2H, $H^{Py\text{-}p}$), 6.50 (m, 4H, $H^{Py\text{-}m}$). – ^{19}F NMR (470 MHz, C_6D_6): δ [ppm] = −132.2 (m, $F^{Ph\text{-}o}$), −157.1 (m, $F^{Ph\text{-}p}$), −163.4 (m, $F^{Ph\text{-}m}$). – ^{13}C{^{1}H} NMR (126 MHz, C_6D_6): δ [ppm] = 148.7 (d, $^1J_{C,F}$ = 246 Hz, C^{Ph}), 146.4 (s, $C^{Py\text{-}o}$), 141.6 (s, $C^{Py\text{-}p}$), 140.4 (d, $^1J_{C,F}$ = 250 Hz, C^{Ph}), 137.6 (d, $^1J_{C,F}$ = 247 Hz, C^{Ph}), 132.8 (s, C2/C7), 132.1 (s, C^q), 132.0 (s, C^q), 128.9 (s, C4/C5), 128.7 (s, C10), 125.6 (s, $C^{Py\text{-}m}$), 125.5 (s, C3/C6), 123.8 (s, C9), 123.5 (s, C^q), 119.1 (m, $C^{Ph\text{-}i}$), 106.4 (s, C≡**C**–B), 100.2 (s, **C**≡C–B). – ^{11}B NMR (160 MHz, C_6D_6): δ [ppm] = −7.0 (s). – Elemental analysis calcd (%) for $C_{52}H_{18}B_2F_{20}N_2$ (M_r = 1072.3): C 58.25, H 1.69, N 2.61; found: C 58.30, H 1.89, N 2.52.

3d·Pym – ^{1}H NMR (500 MHz, C_6D_6): δ [ppm] = 11.75 (s, 1H, N(CH)N), 10.13 (s, 1H, H9), 7.98 (d, 2H, N(C**H**)C), 7.95 (s, 1H, H10), 7.76 (d, $^3J_{H,H}$ = 7.0 Hz, 2H, H2/H7), 7.57 (d, $^3J_{H,H}$ = 8.6 Hz, 2H, H4/H5), 6.99 (dd, $^3J_{H,H}$ = 8.6 Hz, 6.9 Hz, 2H, H3/H6), 5.97 (m, 1H, NCH(C**H**)). – ^{19}F NMR (470 MHz, C_6D_6): δ [ppm] = −131.9 (m, $F^{Ph\text{-}o}$), −153.6 (m, $F^{Ph\text{-}p}$), −161.7 (m, $F^{Ph\text{-}m}$). – ^{13}C{^{1}H} NMR (126 MHz, C_6D_6): δ [ppm] = 157.3 (s, N**C**C oder NCN), 156.3 (s, N**C**C oder NCN), 148.4(d, $^1J_{C,F}$ = 240 Hz, C^{Ph}), 141.4 (d, $^1J_{C,F}$ = 245 Hz, C^{Ph}), 138.0 (d, $^1J_{C,F}$ = 270 Hz, C^{Ph}), 131.66 (s, C^q), 131.30 (s, C^q), 129.9 (s, C2/C7), 129.0 (s, C4/C5), 128.6 (s, C10), 125.6 (s, C3/C6), 124.4 (s, C9), 122.6 (s, C^q), 122.2 (s, NC**C**), 116.10 (m, $C^{Ph\text{-}i}$), 103.3 (s, **C**≡C–B). – ^{11}B NMR (160 MHz, C_6D_6): δ [ppm] = −5.7 (s). – Elemental analysis calcd (%) for $C_{46}H_{12}B_2F_{20}N_2$ (M_r = 994.2): C 55.57, H 1.22, N 2.82; found: C 55.52, H 1.19, N 2.90.

3d·TMEDA – Elemental analysis calcd (%) for $C_{48}H_{24}B_2F_{20}N_2$ (M_r = 1030.3): C 55.96, H 2.35, N 2.72; found: C 56.00, H 2.45, N 2.64.

NMR spectra

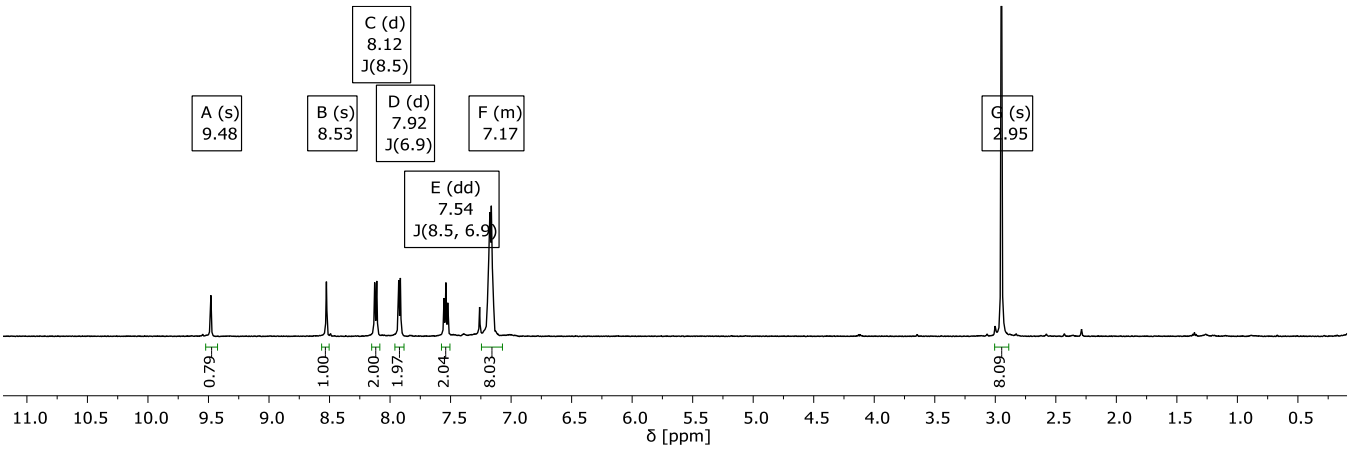

Figure S1. ^{1}H NMR spectrum of **3a** in $CDCl_3$ (500 MHz).

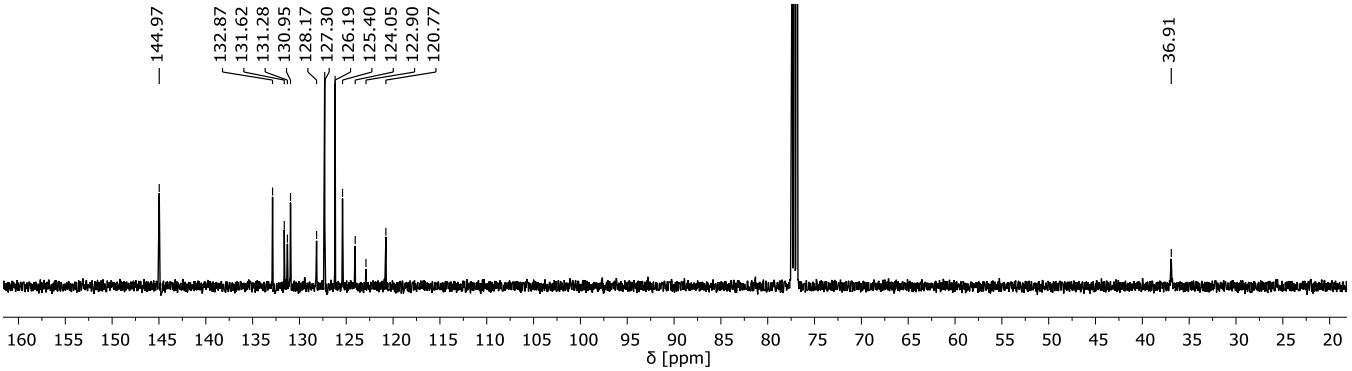

Figure S2. $^{13}C\{^{1}H\}$ NMR spectrum of **3a** in $CDCl_3$ (126 MHz).

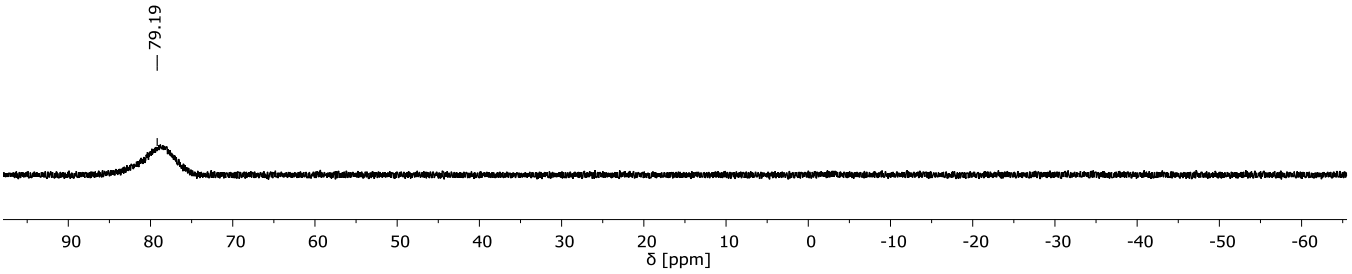

Figure S3. ^{11}B NMR spectrum of **3a** in $CDCl_3$ (160 MHz).

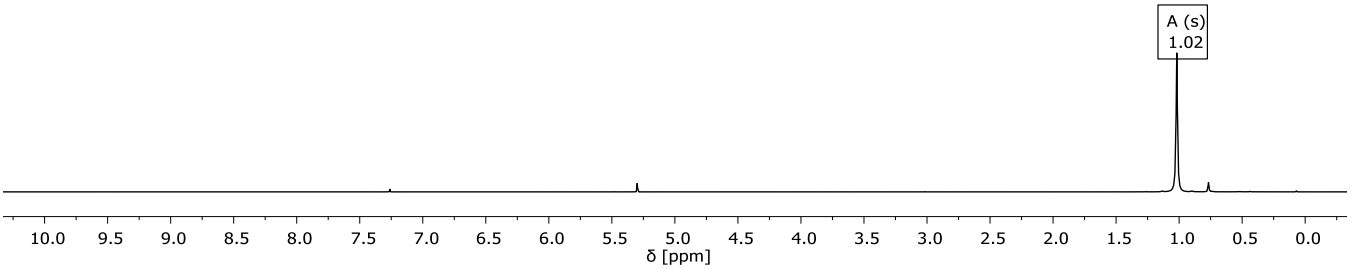

Figure S4. ^{1}H NMR spectrum of Me_2BCl (**2b**) in $CDCl_3$ (500 MHz).

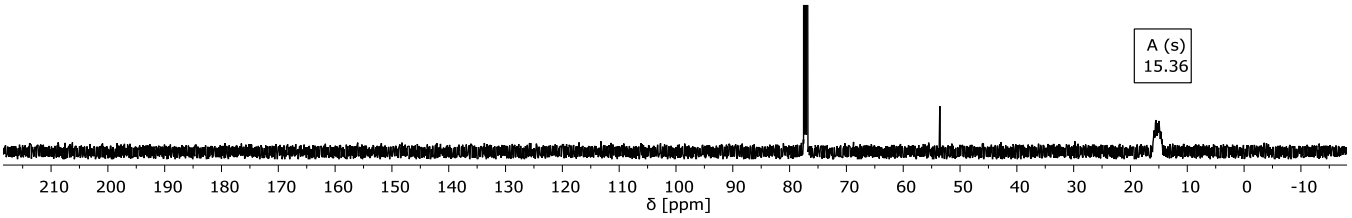

Figure S5. $^{13}C\{^{1}H\}$ NMR spectrum of Me_2BCl (**2b**) in $CDCl_3$ (126 MHz).

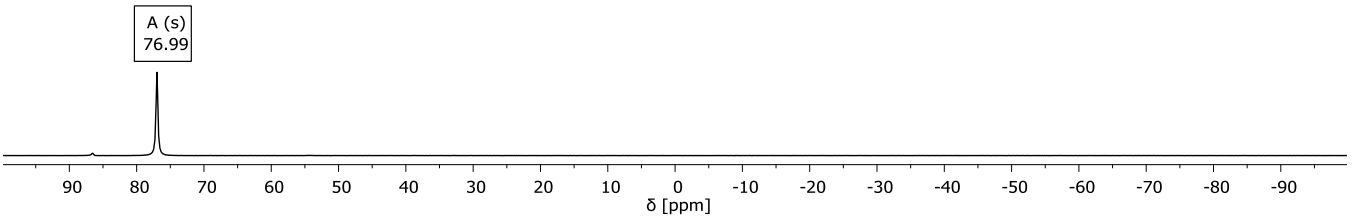

Figure S6. ^{11}B NMR spectrum of Me_2BCl (**2b**) in $CDCl_3$ (160 MHz).

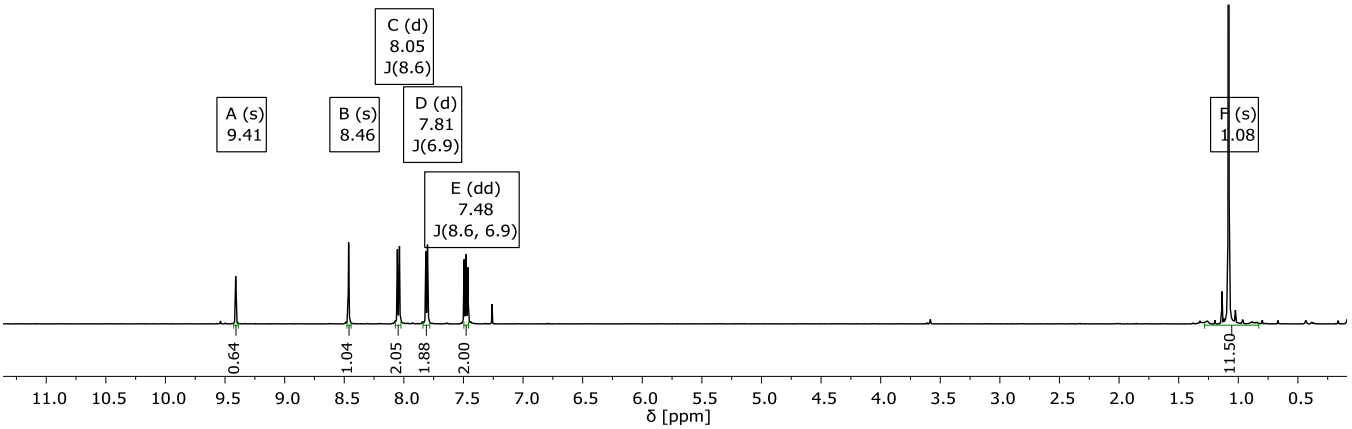

Figure S7. ^{1}H NMR spectrum of **3b** in $CDCl_3$ (500 MHz).

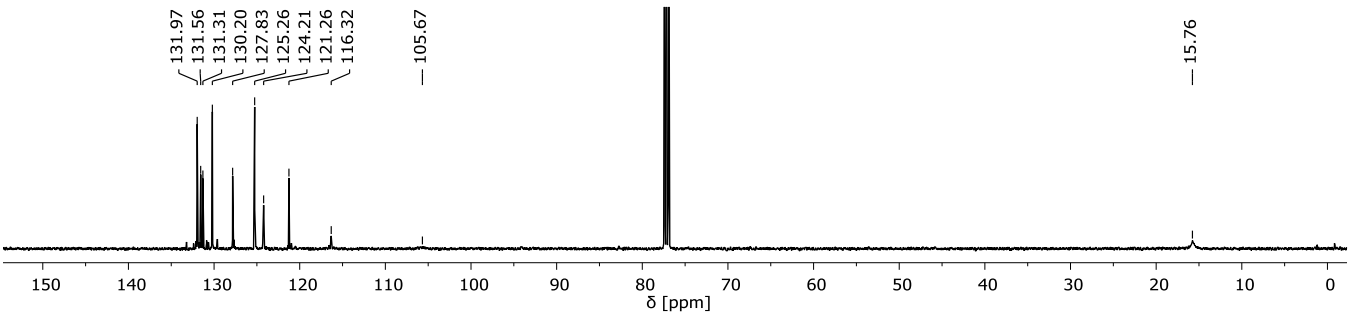

Figure S8. $^{13}C\{^{1}H\}$ NMR spectrum of **3b** in $CDCl_3$ (126 MHz).

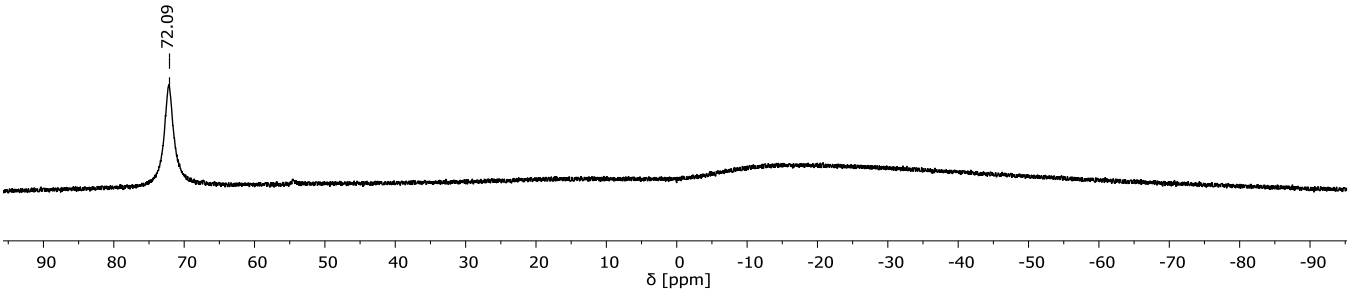

Figure S9. ^{11}B NMR spectrum of **3b** in $CDCl_3$ (160 MHz).

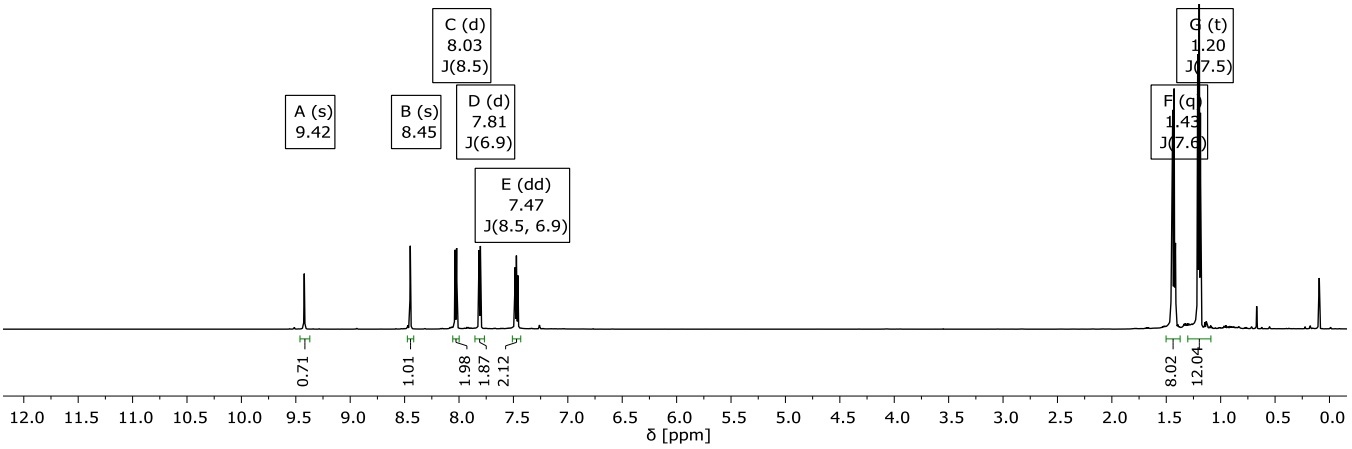

Figure S10. ^{1}H NMR spectrum of **3c** in $CDCl_3$ (600 MHz).

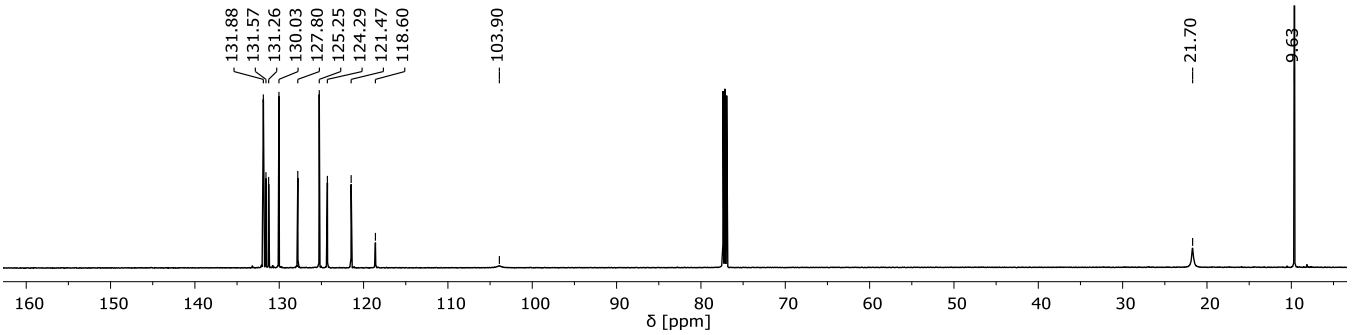

Figure S11. $^{13}C\{^{1}H\}$ NMR spectrum of **3c** in $CDCl_3$ (150 MHz).

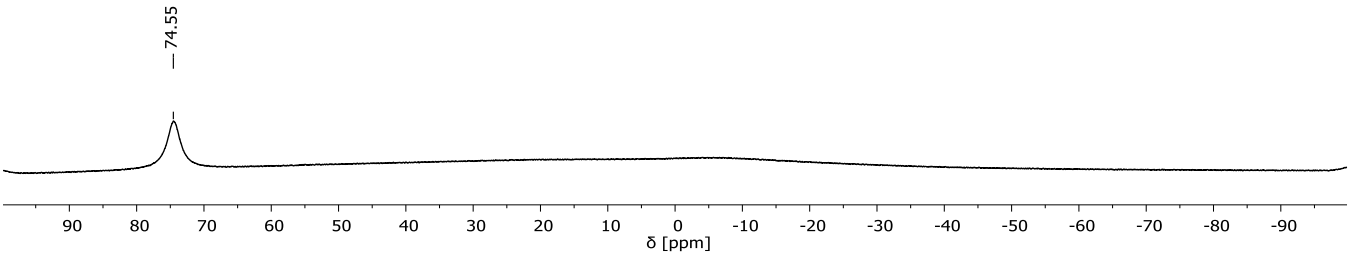

Figure S12. ^{11}B NMR spectrum of **3c** in $CDCl_3$ (160 MHz).

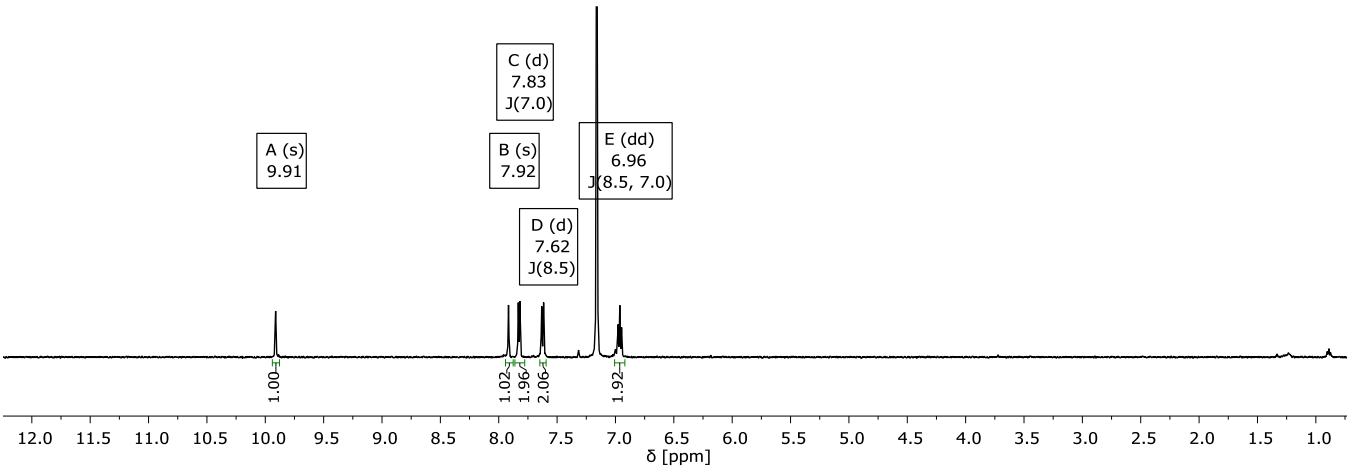

Figure S13. ^{1}H NMR spectrum of **3d** in C_6D_6 (500 MHz).

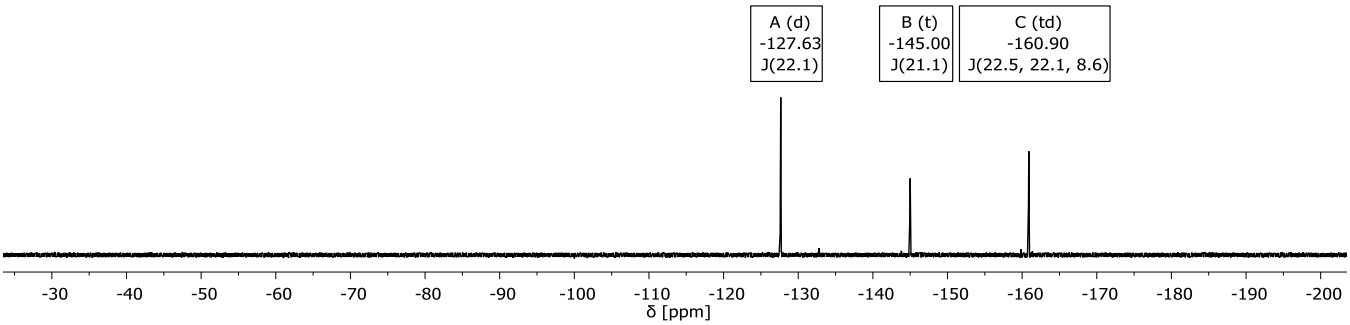

Figure S14. ^{19}F NMR spectrum of **3d** in C_6D_6 (470 MHz).

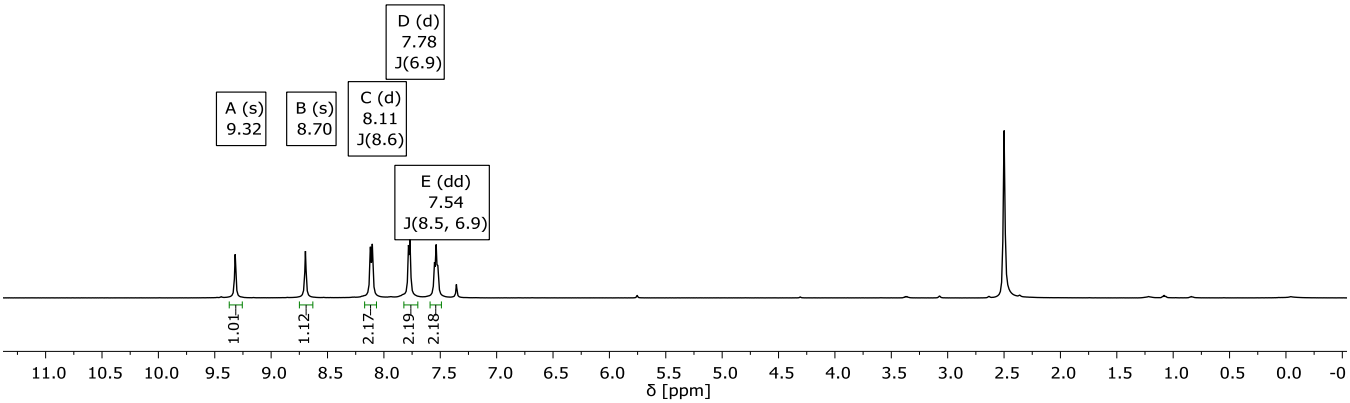

Figure S15. ^{1}H NMR spectrum of **3d** in DMSO-d_6 (500 MHz).

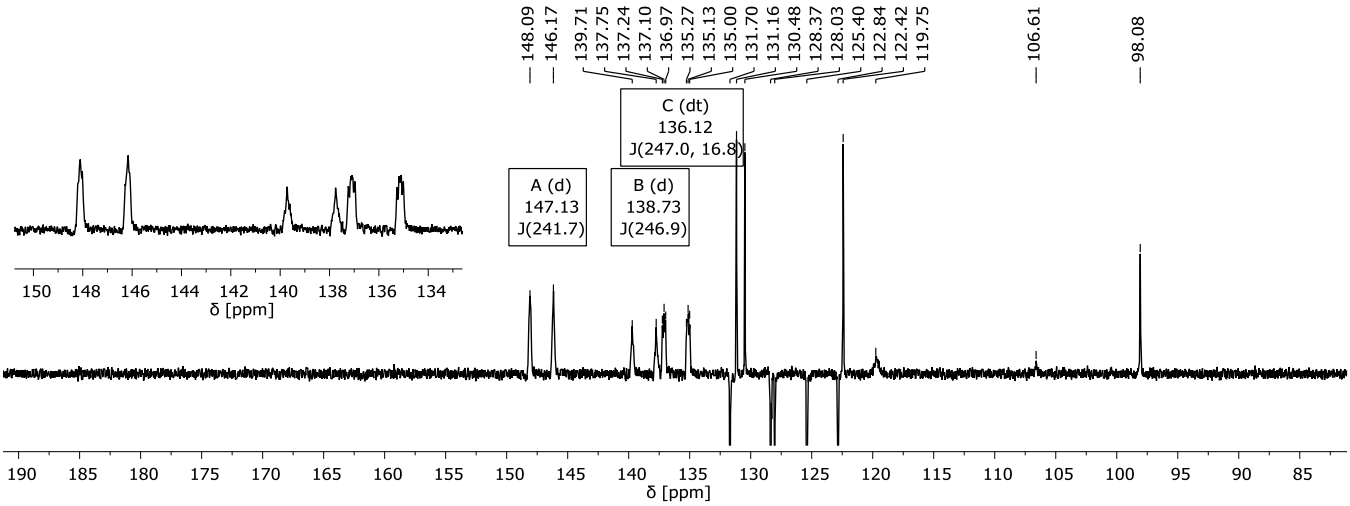

Figure S16. $^{13}C\{^{1}H\}$ DEPT NMR spectrum of **3d** in DMSO-d_6 (126 MHz).

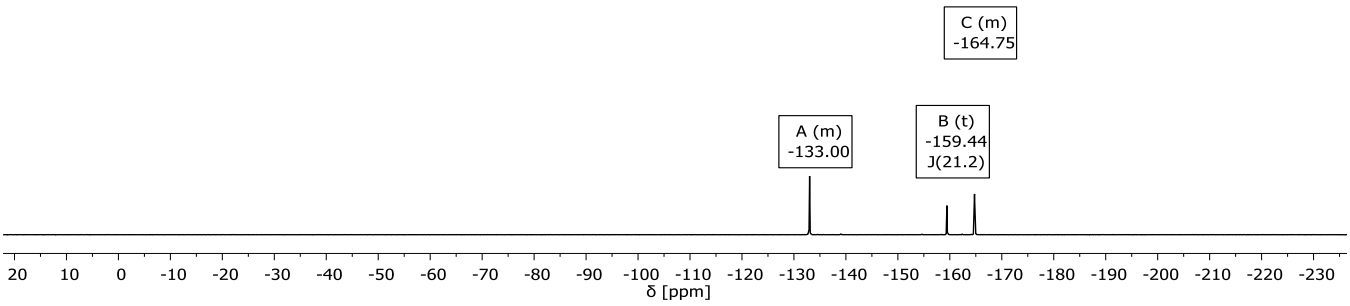

Figure S17. ^{19}F NMR spectrum of **3d** in DMSO-d_6 (470 MHz).

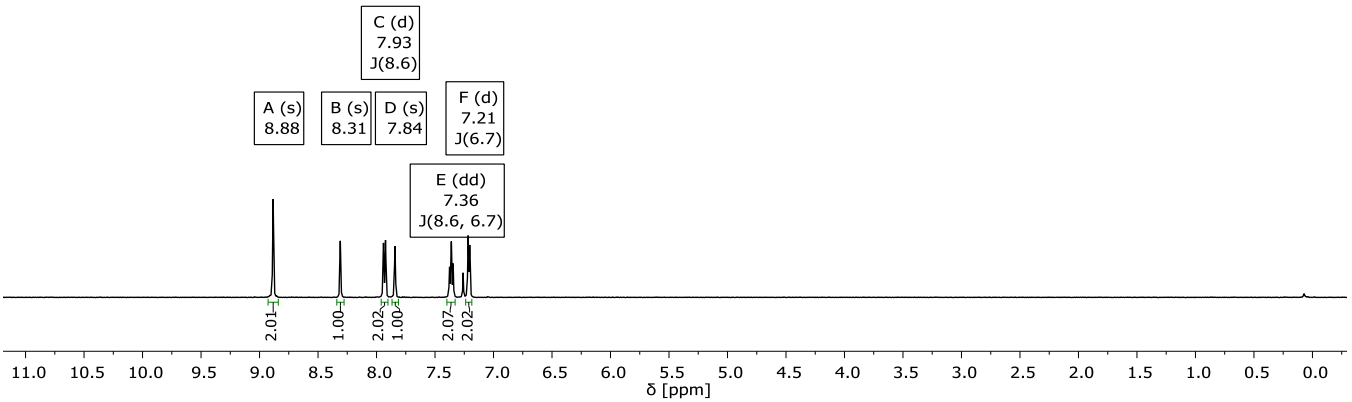

Figure S18. ^{1}H NMR spectrum of **4d** in $CDCl_3$ (500 MHz).

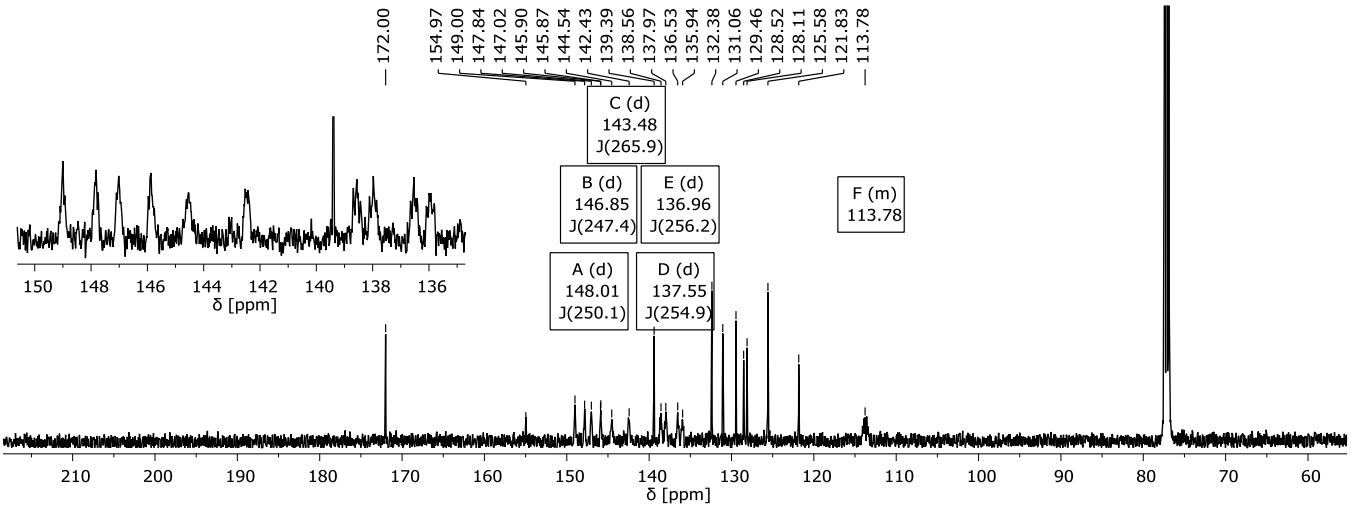

Figure S19. $^{13}C\{^{1}H\}$ NMR spectrum of **4d** in $CDCl_3$ (126 MHz).

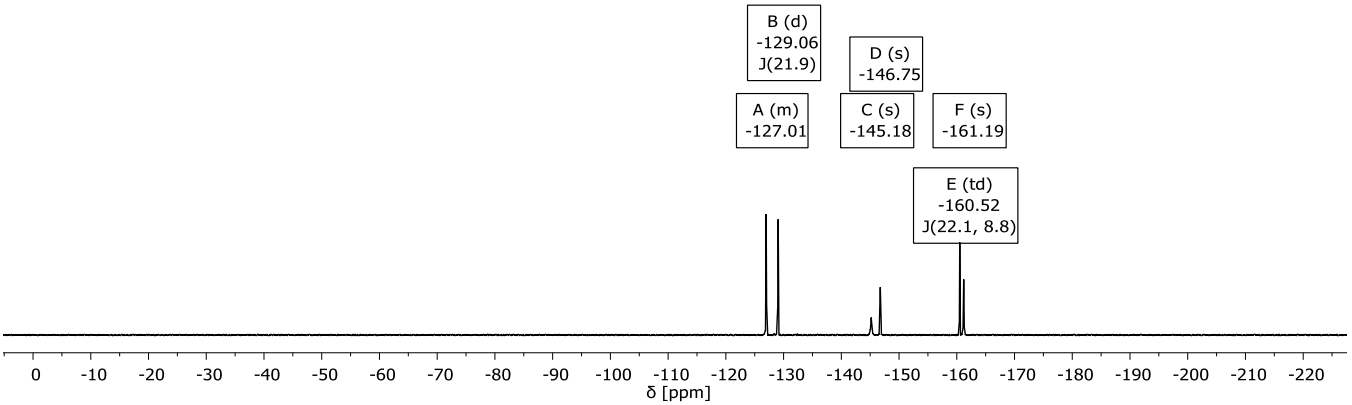

Figure S20. ^{19}F NMR spectrum of **4d** in $CDCl_3$ (470 MHz).

NMR spectra of the adducts

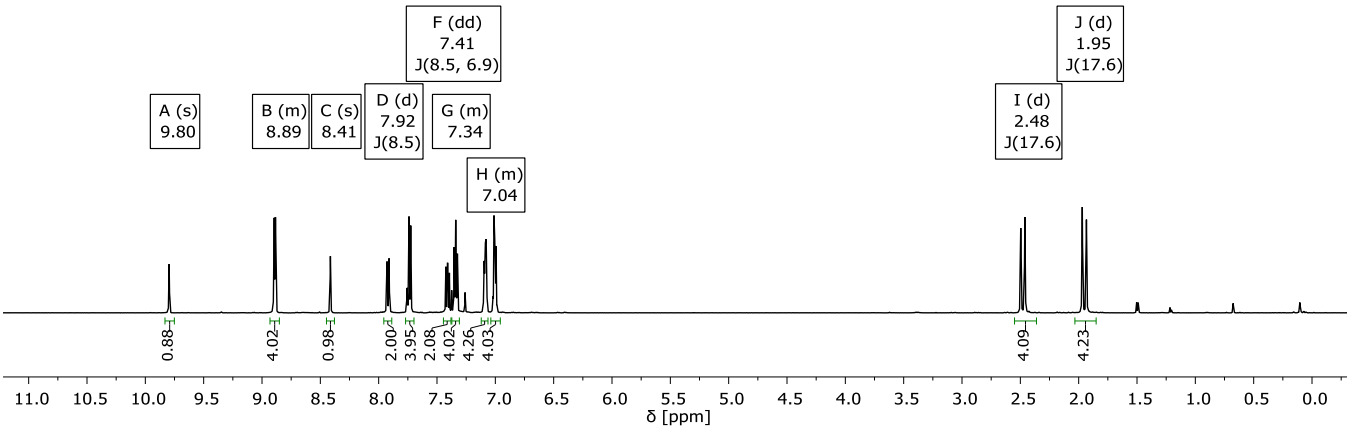

Figure S21. ^{1}H NMR spectrum of **3a**·2 Py in $CDCl_3$ (500 MHz).

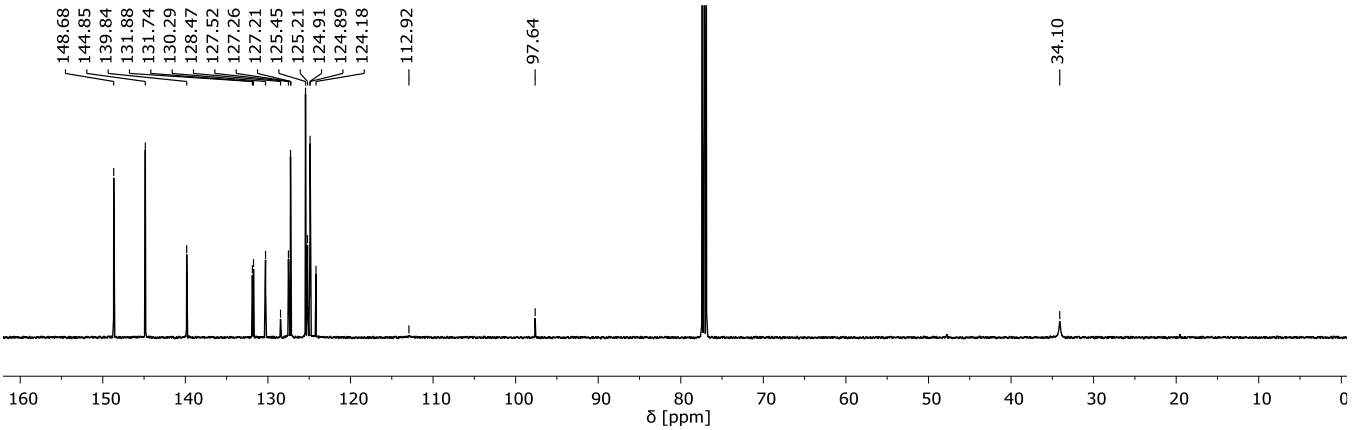

Figure S22. $^{13}C\{^{1}H\}$ NMR spectrum of **3a**·2 Py in $CDCl_3$ (126 MHz).

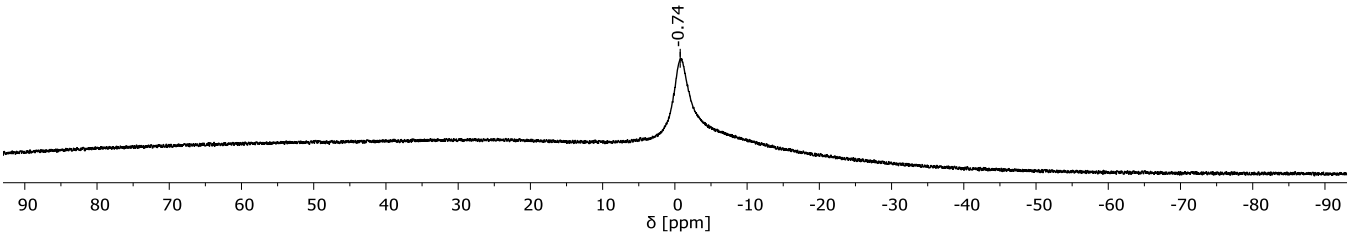

Figure S23. ^{11}B NMR spectrum of **3a**·2 Py in $CDCl_3$ (160 MHz).

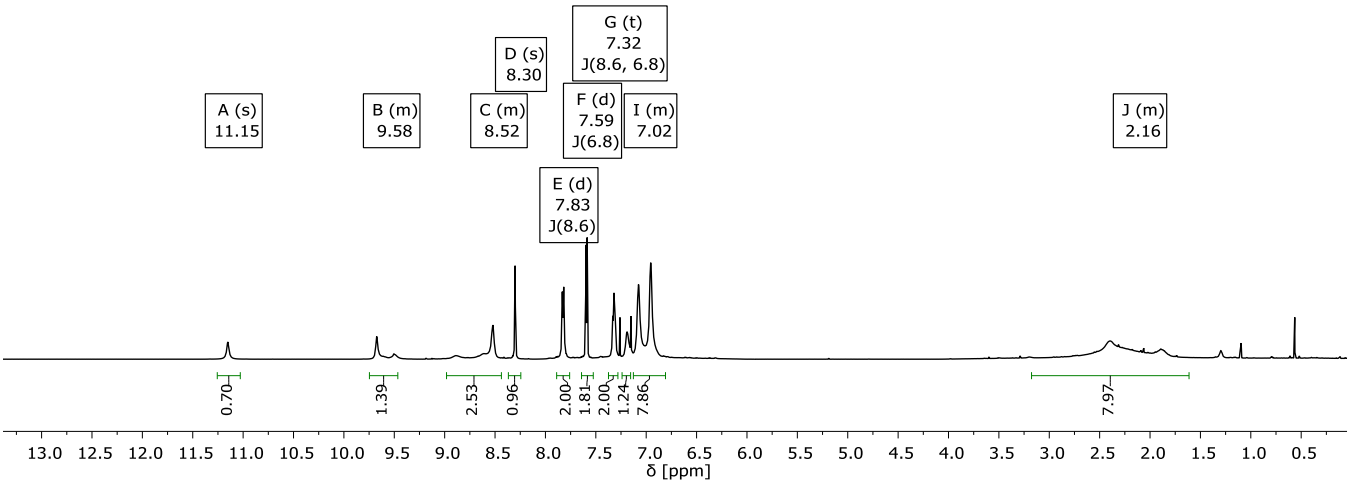

Figure S24. ^{1}H NMR spectrum of **3a**·Pym in $CDCl_3$ (600 MHz).

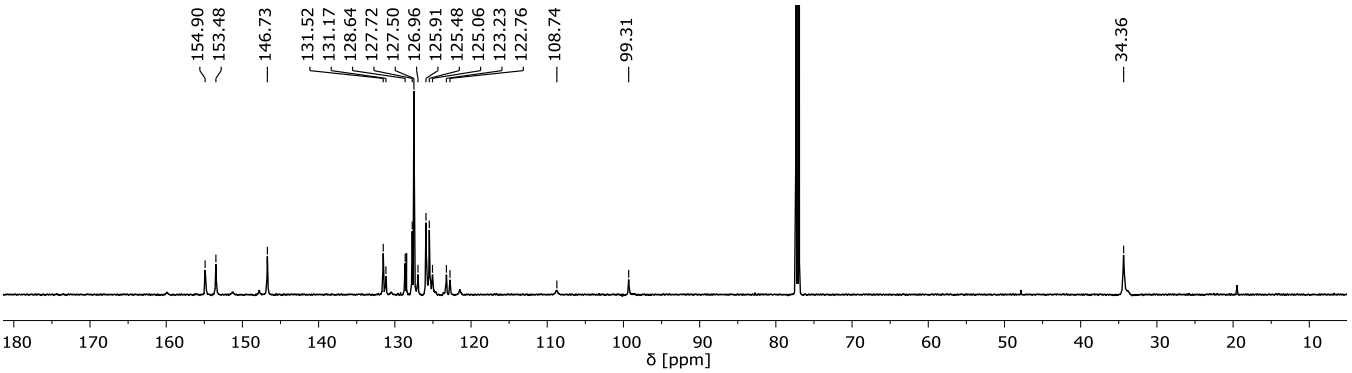

Figure S25. $^{13}C\{^{1}H\}$ NMR spectrum of **3a**·Pym in $CDCl_3$ (150 MHz).

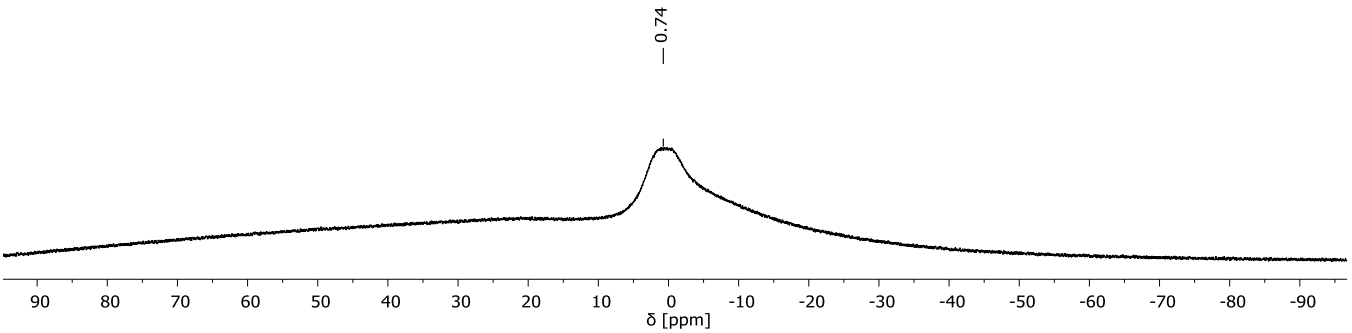

Figure S26. ^{11}B NMR spectrum of **3a**·Pym in $CDCl_3$ (160 MHz).

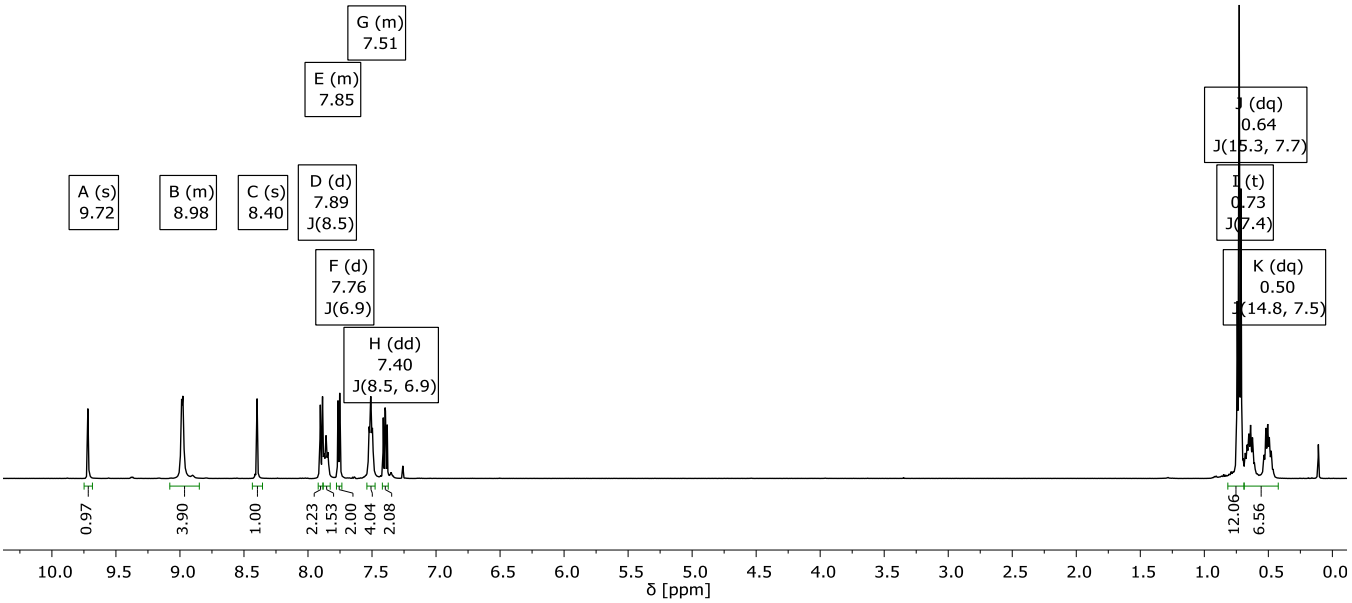

Figure S27. ^{1}H NMR spectrum of **3c**·2 Py in $CDCl_3$ (500 MHz).

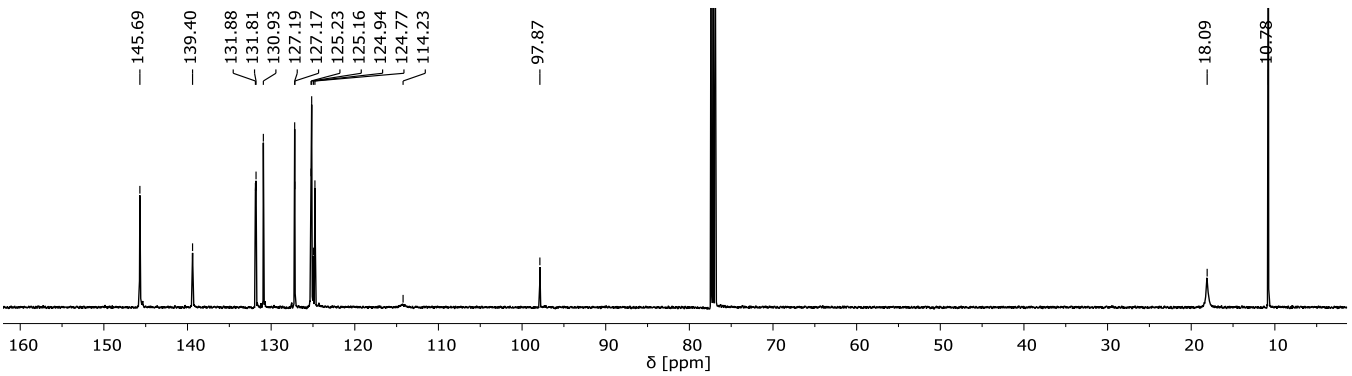

Figure S28. $^{13}C\{^{1}H\}$ NMR spectrum of **3c**·2 Py in $CDCl_3$ (126 MHz).

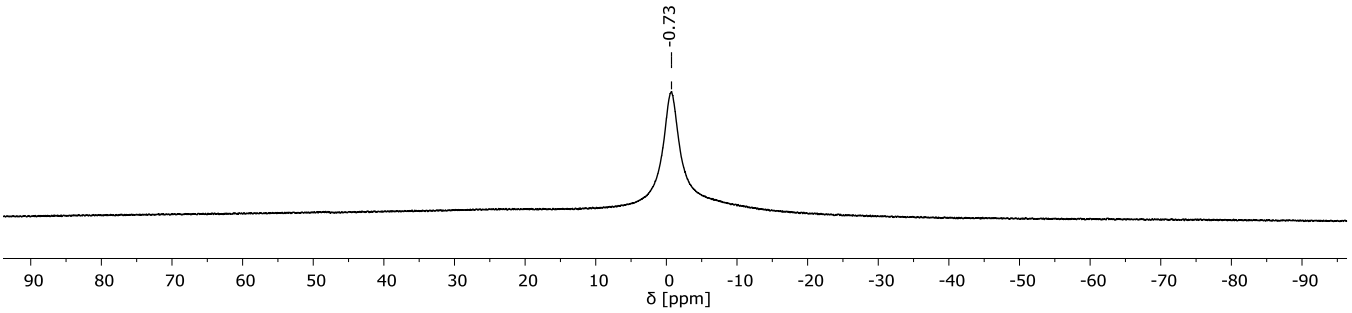

Figure S29. ^{11}B NMR spectrum of **3c**·2 Py in $CDCl_3$ (160 MHz).

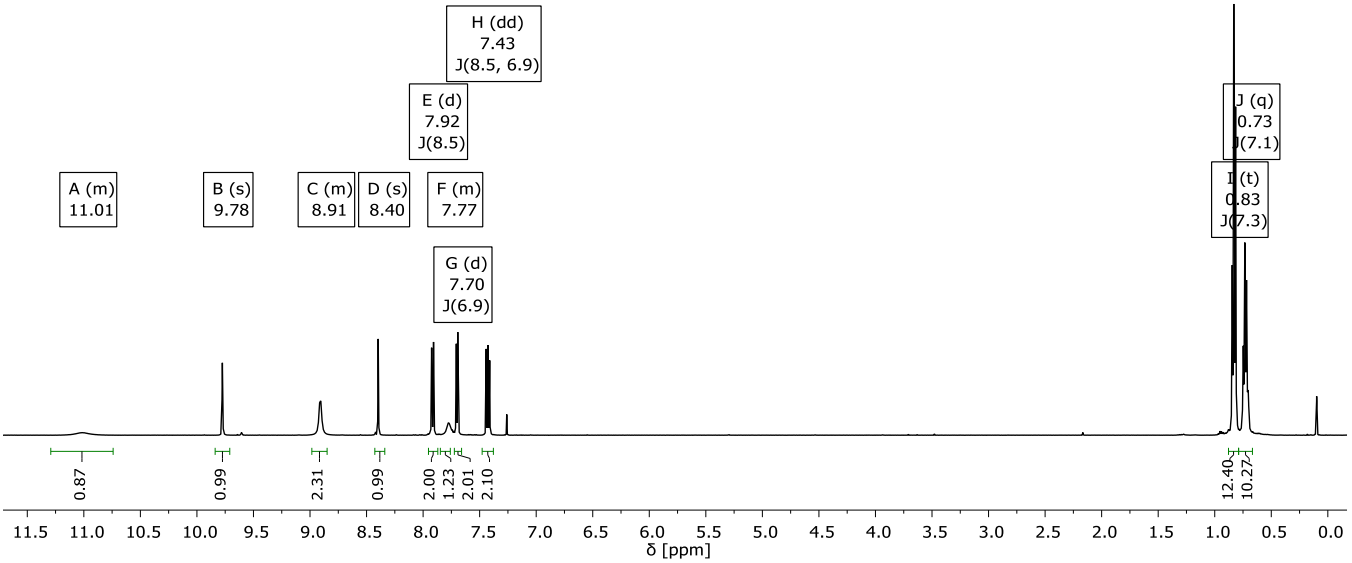

Figure S30. ^{1}H NMR spectrum of **3c**·Pym in $CDCl_3$ (500 MHz).

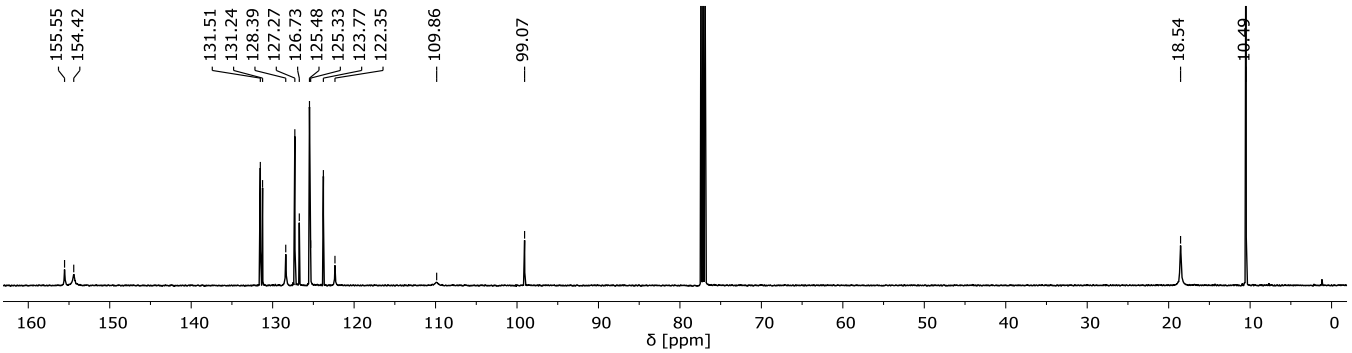

Figure S31. $^{13}C\{^{1}H\}$ NMR spectrum of **3c**·Pym in $CDCl_3$ (126 MHz).

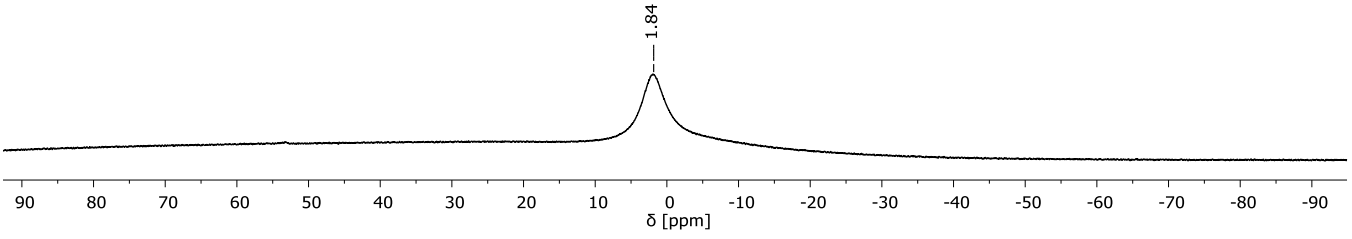

Figure S32. ^{11}B NMR spectrum of **3c**·Pym in $CDCl_3$ (160 MHz).

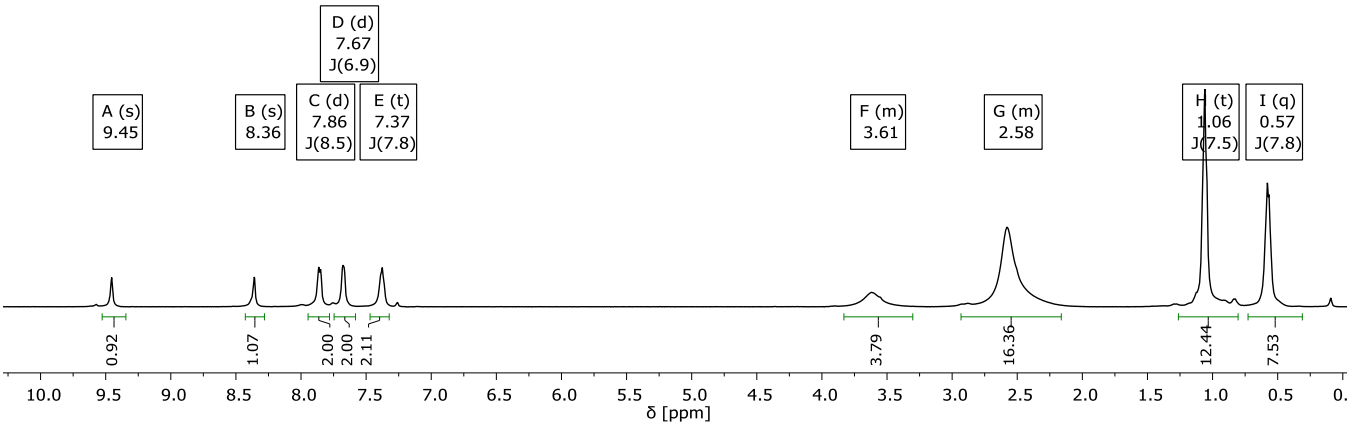

Figure S33. ^{1}H NMR spectrum of **3c**·TMEDA in $CDCl_3$ (500 MHz).

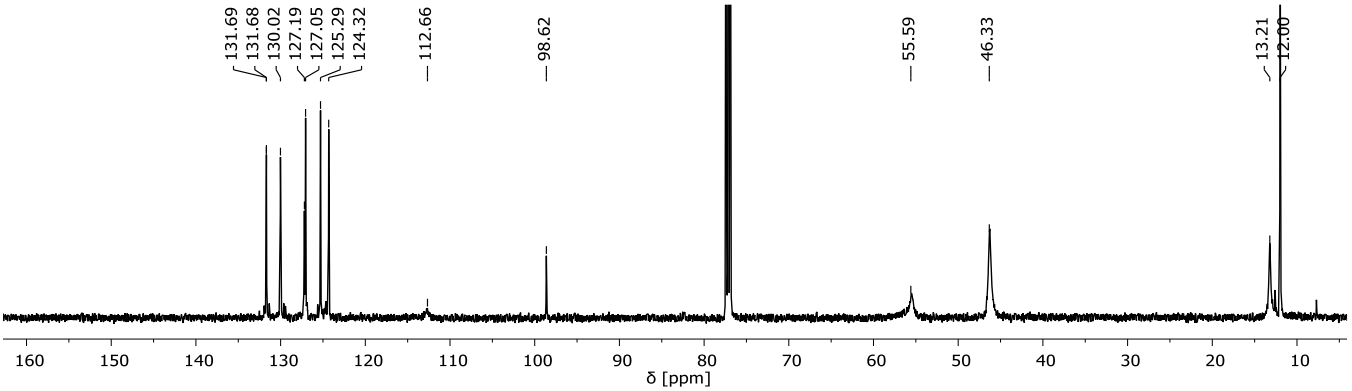

Figure S34. $^{13}C\{^{1}H\}$ NMR spectrum of **3c**·TMEDA in $CDCl_3$ (126 MHz).

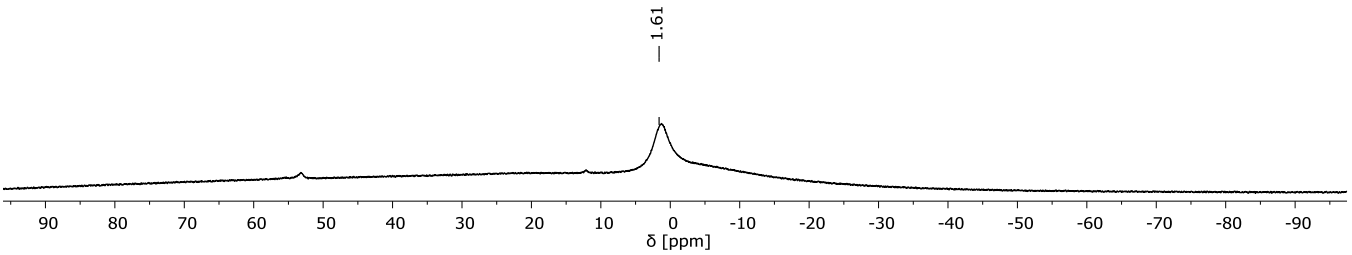

Figure S35. ^{11}B NMR spectrum of **3c**·TMEDA in $CDCl_3$ (160 MHz).

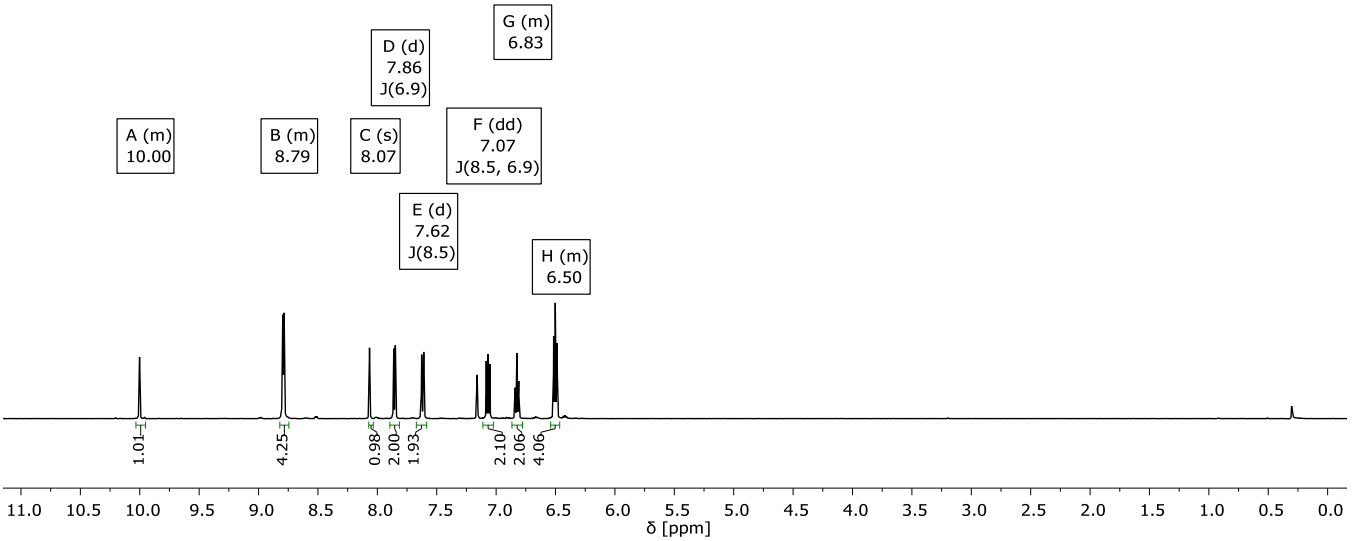

Figure S36. ^{1}H NMR spectrum of **3d**·2 Py in C_6D_6 (500 MHz).

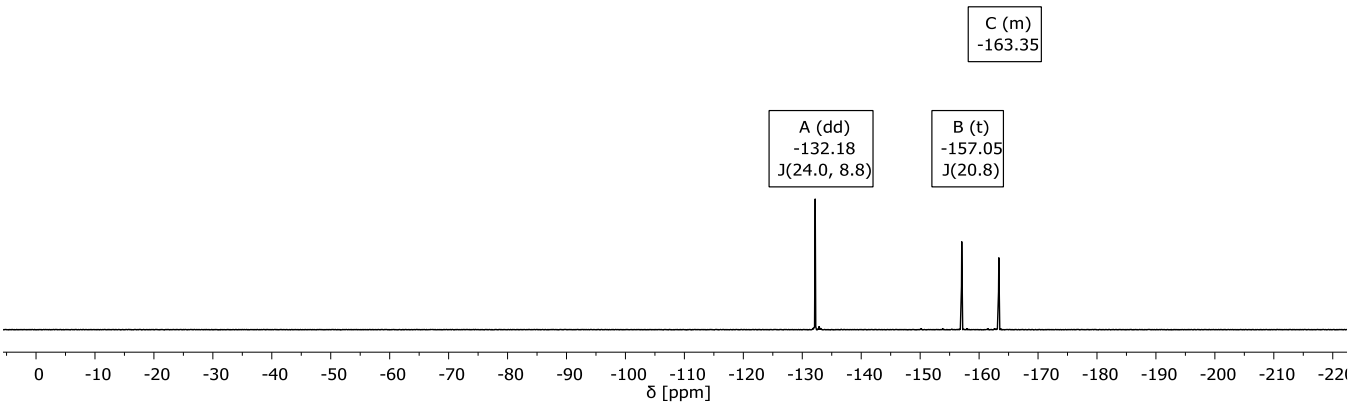

Figure S37. ^{19}F NMR spectrum of **3d**·2 Py in C_6D_6 (470 MHz).

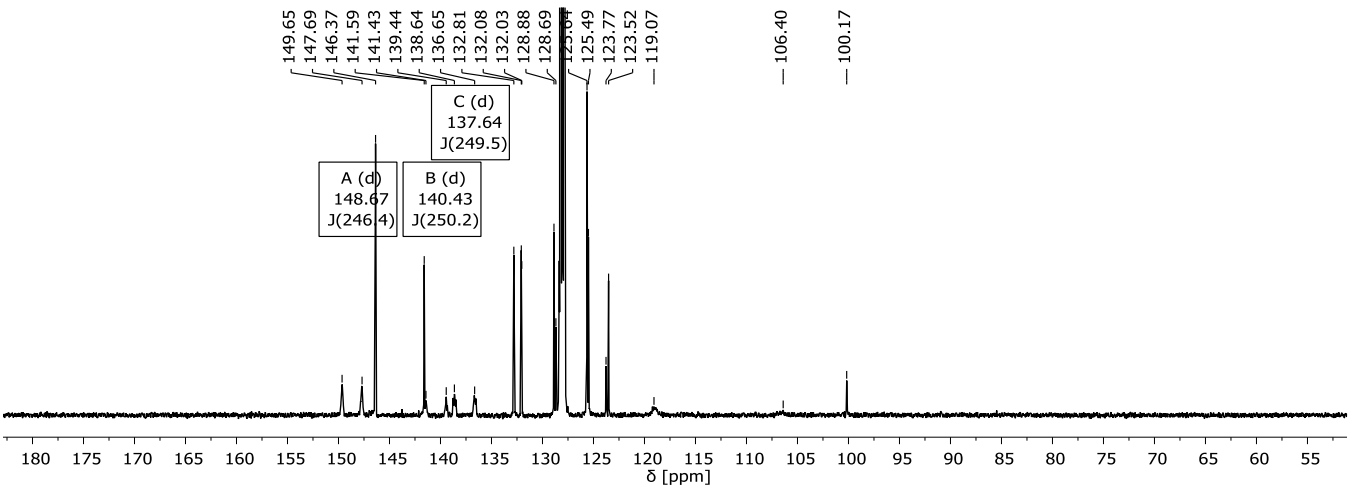

Figure S38. ^{13}C NMR spectrum of **3d**·2 Py in C_6D_6 (126 MHz).

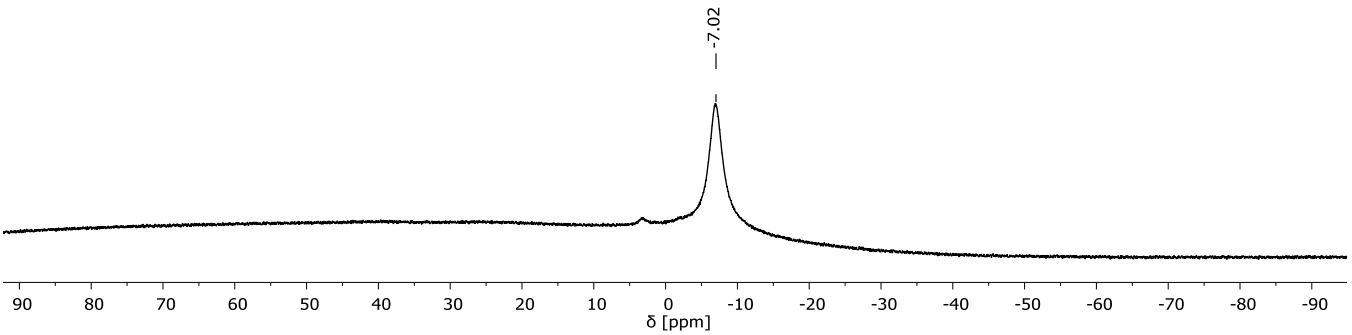

Figure S39. ^{11}B NMR spectrum of **3d**·2 Py in C_6D_6 (160 MHz).

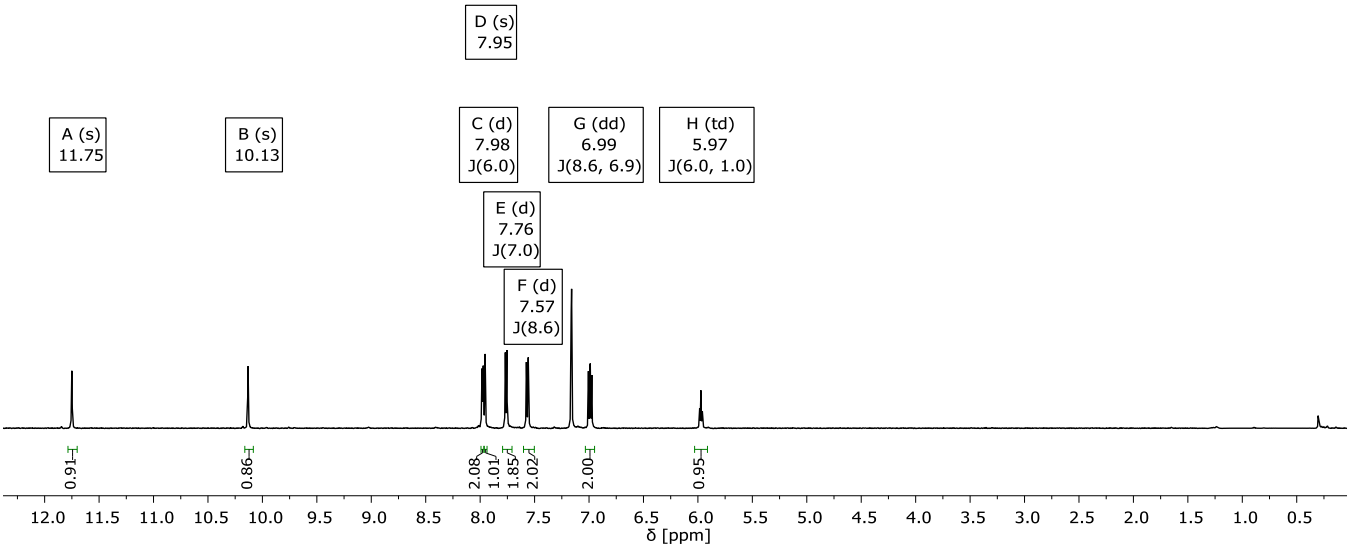

Figure S40. ^{1}H NMR spectrum of **3d**·Pym in C_6D_6 (500 MHz).

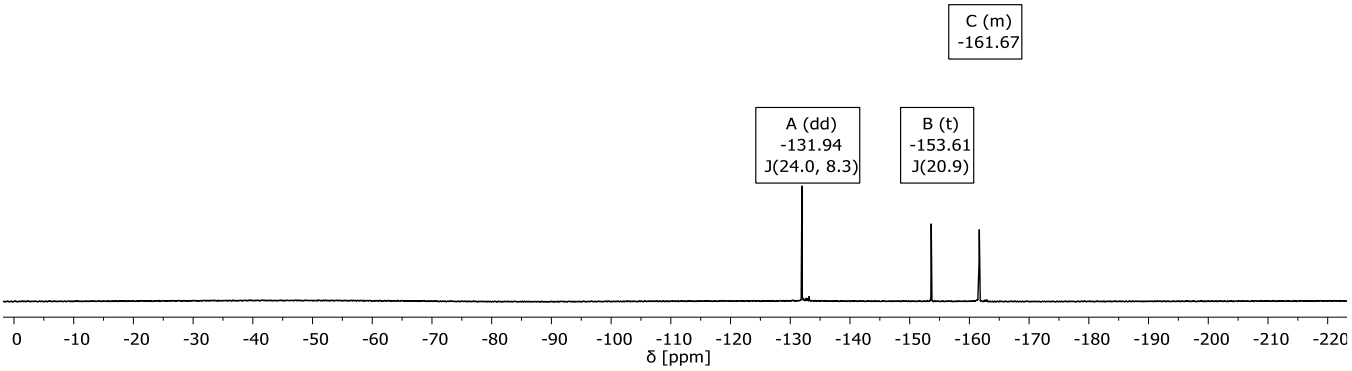

Figure S41. ^{19}F NMR spectrum of **3d**·Pym in C_6D_6 (470 MHz).

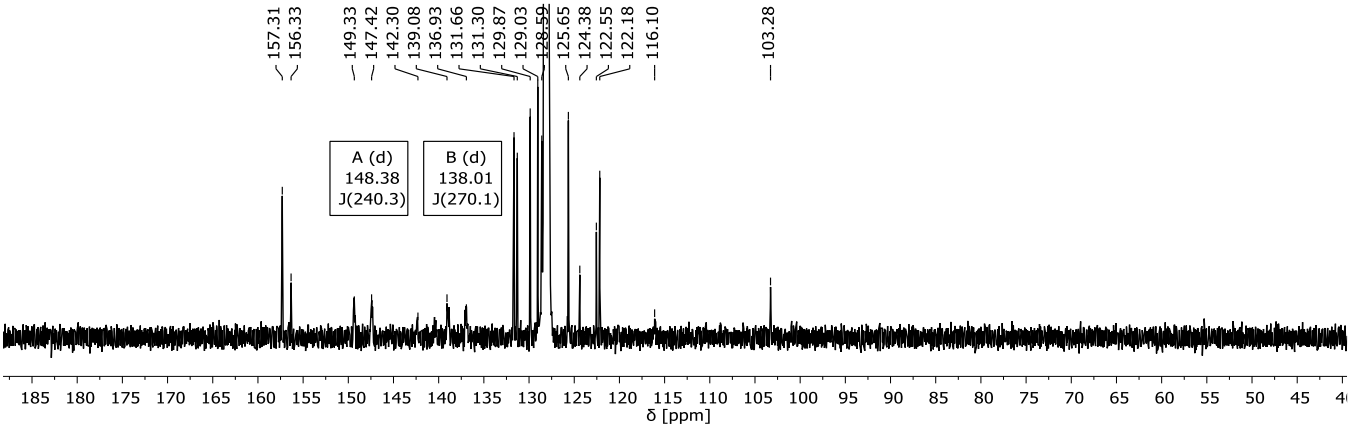

Figure S42. ^{13}C NMR spectrum of **3d**·Pym in C_6D_6 (126 MHz).

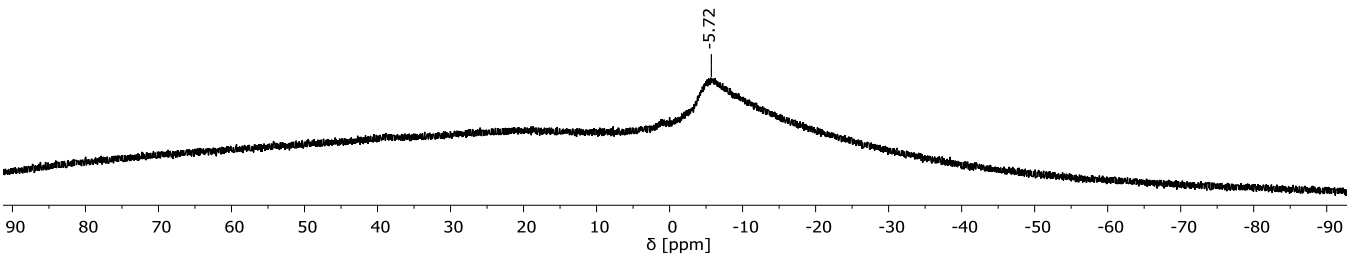

Figure S43. ^{11}B NMR spectrum of **3d**·Pym in C_6D_6 (160 MHz).

Solid state structures of 2-(diisopropylamino)-2-boraindane and bis(2-methylphenyl)-diisopropylaminoborane

During preparation of 2-chloro-2-boraindane diethyl etherate (**2a**) according to a literature protocol,[2] single crystals of the precursor 2-(diisopropylamino)-2-boraindane (**I**) and the by-product diisopropylamino-bis(2-methylbenzyl)borane (**II**) were obtained (Scheme S2). Solid state structures of both compounds were determined by single crystal X-ray diffraction. The structures of **I** and **II** are shown in Figure S44.

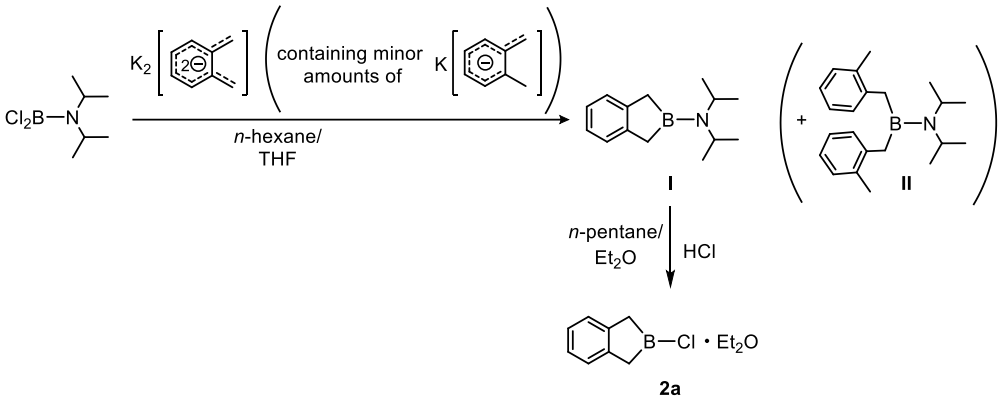

Scheme S2. Generation of the compounds **I** and **II** during the synthesis of 2-chloro-2-boraindane diethyl etherate (**2a**)

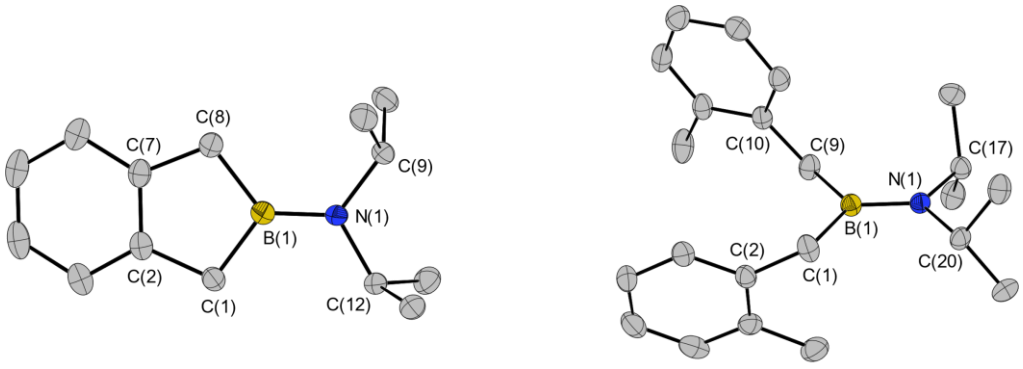

I **II**

Figure S44. Molecular structures of **I** and **II** in the solid state. Hydrogen atoms are omitted for clarity. For **I**, one of two independent molecules in the asymmetric unit is shown. Ellipsoids are set at 50% probability. Selected distances [Å] and angles [°] of **I**: B(1)–N(1) 1.391(1), N(1)–C(9) 1.485(1), N(1)–C(12) 1.481(1), B(1)–C(1) 1.601(1), B(1)–C(8) 1.603(1), C(1)–C(2) 1.514(1), C(7)–C(8) 1.518(1); C(9)–N(1)–B(1) 125.3(1), C(12)–N(1)–B(1) 120.5(1), C(9)–N(1)–C(12) 114.2(1), N(1)–B(1)–C(1) 125.2(1), N(1)–B(1)–C(8) 127.9(1), C(1)–B(1)–C(8) 106.9(1), B(1)–C(1)–C(2) 103.5(1), B(1)–C(8)–C(7) 103.5(1); of **II**: B(1)–N(1) 1.407(2), N(1)–C(17) 1.485(1), N(1)–C(20) 1.484(1), B(1)–C(1) 1.607(2), B(1)–C(9) 1.594(2), C(1)–C(2) 1.510(2), C(9)–C(10) 1.513(2); C(17)–N(1)–B(1) 124.8(1), C(20)–N(1)–B(1) 122.5(1), C(17)–N(1)–C(20) 112.7(1), N(1)–B(1)–C(1) 121.5(1), N(1)–B(1)–C(9) 123.7(1), B(1)–C(1)–C(2) 114.0(1), B(1)–C(9)–C(10) 113.9(1).

Crystallographic data

Single crystals were examined on a Rigaku Supernova diffractometer. The crystals were kept at 100.0(1) K during data collection. Using Olex2[7], the structures were solved with the ShelXT[8] structure solution program using Intrinsic Phasing and refined with the ShelXL[9] or olex2.refine[10] refinement package using Least Squares minimization.

[**3a**·2 Py] was refined as a racemic twin and a disorder of C61 to C68 over two sites was modelled with ratio 82:18. For the refinement of [**3c**·2 Py] and [**3c**·TMEDA]**,** non-spherical atom-form factors were applied using NoSpherA2.[11] The crystal of [**3c**·TMEDA] was non-merohedrically twinned, the second domain was rotated by 42.1° around [0.97 0.22 -0.08] (reciprocal) or [0.98 0.18 0.04] (direct) with ratio 92:8. Both domains were taken into account for data reduction and refinement. In [**3d**·2 Py], one C_6F_6 groups is disordered with ratio 47:53, rigid body restraints were applied to disordered atoms. The crystal of [**4d**·2.5 C_6H_6] was non-merohedrically twinned, approximate ratio 60:40. Both domains were taken into account during data reduction, only the reflections of the main domain and the composite ones were used for structure refinement.

Details of the X-ray investigation are given in Table S1, Table S2 and Table S3. CCDC 2337388 – 2337399 contain the supplementary crystallographic data for this paper. These data can be obtained free of charge from The Cambridge Crystallographic Data Centre via https://www.ccdc.cam.ac.uk/structures.

Table S1. Crystallographic data for compounds **3a**, **3d**, **4d** and [**3d**·2 Py].

Compound	**3a**	**3d**	[**4d**·2.5 C_6H_6]	[**3d**·2 Py]
Empirical formula	$C_{34}H_{24}B_2$	$C_{42}H_8B_2F_{20}$	$C_{81}H_{25}B_4F_{40}$	$C_{58}H_{24}B_2F_{20}N_2$
M_r	454.15	914.10	1801.25	1150.41
T [K]	99.9(3)	100.0(1)	100.0(1)	100.0(1)
Radiation	Cu Kα	Cu Kα	Cu Kα	Cu Kα
Crystal system	monoclinic	monoclinic	triclinic	triclinic
Space group	$P2_1/n$	$P2_1/n$	$P\bar{1}$	$P\bar{1}$
a [Å]	5.00408(14)	19.8509(2)	12.7646(9)	11.3707(7)
b [Å]	20.9765(5)	7.70443(10)	16.0907(10)	12.0641(7)
c [Å]	23.1586(6)	22.3199(3)	19.4943(13)	19.7225(10)
α [°]	90	90	80.332(5)	105.644(5)
β [°]	92.490(2)	96.0176(10)	71.304(6)	96.165(5)
γ [°]	90	90	69.470(6)	108.009(5)
Volume [Å^3]	2428.62(11)	3394.80(7)	3544.8(4)	2423.3(3)
Z	4	4	2	2
ρ_{calc} [g cm^{-3}]	1.242	1.789	1.688	1.577
μ [mm^{-1}]	0.520	1.629	1.545	1.289
F(000) [e]	952	1800	1782	1152
2Θ range [°]	5.686 – 152.996	5.67 – 152.74	5.876 – 148.274	8.002 – 136.502
	$-6 \le h \le 5$	$-25 \le h \le 25$	$-15 \le h \le 15$	$-13 \le h \le 13$
Index ranges	$-17 \le k \le 26$	$-9 \le k \le 9$	$-19 \le k \le 19$	$-14 \le k \le 13$
	$-27 \le l \le 28$	$-28 \le l \le 28$	$-24 \le l \le 18$	$-22 \le l \le 23$
Refl. collected	14521	56830	25292	32253
Independent refl.	5007	7084	14816	8872
R_{int}	0.0305	0.0297	0.0853	0.1250
Refl. with $I > 2\sigma(I)$	4586	6380	10457	4899
Data / restraints / parameters	5007 / 0 / 421	7084 / 0 / 577	14816 / 0 / 1128	8872 / 162 / 827
Goodness-of-Fit on F^2	1.037	1.026	0.944	1.004
R_1/wR_2 [$I > 2\sigma(I)$]	0.0424 / 0.1116	0.0303 / 0.0809	0.0592 / 0.1479	0.0632 / 0.1344
R_1/wR_2 (all data)	0.0458 / 0.1149	0.0340 / 0.0844	0.0807 / 0.1563	0.1279 / 0.1731
ρ_{fin} (max/min) [e Å^{-3}]	0.28 / −0.18	0.26 / −0.20	0.46 / −0.33	0.29 / −0.32
CCDC	2337388	2337389	2337390	2337391

Table S2. Crystallographic data for compounds [**3a**·2 Py], [**3a**·TMEDA], [**3c**·2 Py] and [**3c**·Pym].

Compound	[**3a**·2 Py]	[**3a**·TMEDA]	[**3c**·2 Py]	[**3c**·Pym]·C_6H_6
Empirical formula	$C_{44}H_{34}B_2N_2$	$C_{40}H_{40}B_2N_2$	$C_{36}H_{38}B_2N_2$	$C_{36}H_{38}B_2N_2$
M_r	612.35	570.36	520.365	520.30
T [K]	100.0(1)	100.0(1)	100.0(1)	100.0(1)
Radiation	Cu Kα	Cu Kα	Mo Kα	Cu Kα
Crystal system	monoclinic	monoclinic	monoclinic	monoclinic
Space group	$P2_1$	$P2_1/n$	$P2_1/c$	$P2_1/n$
a [Å]	11.17085(16)	10.3734(3)	11.8924(3)	10.5387(1)
b [Å]	18.4947(2)	19.5963(5)	16.8358(3)	20.1073(2)
c [Å]	16.5929(2)	15.8553(3)	16.0803(3)	14.4086(2)
β [°]	101.4546(14)	102.198(2)	110.959(2)	103.080(2)
Volume [Å^3]	3359.85(8)	3150.28(13)	3006.55(12)	2974.03(6)
Z	4	4	4	4
ρ_{calc} [g cm^{-3}]	1.211	1.203	1.150	1.162
μ [mm^{-1}]	0.525	0.514	0.065	0.496
F(000) [e]	1288	1216	1112.3	1112
2Θ range [°]	5.434 – 152.652	7.272 – 153.556	5.54 to 73.74	7.682 – 152.906
Index ranges	$-14 \le h \le 14$ $-22 \le k \le 23$ $-20 \le l \le 20$	$-12 \le h \le 12$ $-17 \le k \le 24$ $-19 \le l \le 19$	-19 ≤ h ≤ 19 -27 ≤ k ≤ 28 -27 ≤ l ≤ 26	$-13 \le h \le 13$ $-25 \le k \le 25$ $-16 \le l \le 17$
Refl. collected	65174	30802	95727	65556
Independent refl.	13796	6535	14575	6218
R_{int}	0.0290	0.0408	0.0384	0.0355
Refl. with $I > 2\sigma(I)$	13520	5057	11136	5463
Data / restraints / parameters	13796/1/891	6535 / 0 / 558	14575/0/703	6218 / 0 / 365
Goodness-of-Fit on F^2	1.130	1.013	1.083	1.042
R_1/wR_2 [$I > 2\sigma(I)$]	0.0687 / 0.1791	0.0402 / 0.0946	0.0347 / 0.0680	0.0412 / 0.1067
R_1/wR_2 (all data)	0.0697 / 0.1800	0.0580 / 0.1048	0.0545, wR_2 = 0.0751	0.0473 / 0.1114
ρ_{fin} (max/min) [e Å^{-3}]	0.53 / −0.28	0.21 / −0.19	0.38 /-0.24	0.25 / −0.19
CCDC	2337392	2337393	2337394	2337395

Table S3. Crystallographic data for compounds [**3c**·TMEDA], [**3d**·Pym], **I** and **II**.

Compound	[**3c**·TMEDA]	[**3d**·Pym]	**I**	**II**
Empirical formula	$C_{32}H_{44}B_2N_2$	$C_{46}H_{12}B_2N_2F_{20}$	$C_{14}H_{22}BN$	$C_{22}H_{32}BN$
M_r	478.37	994.20	215.13	321.29
T [K]	100.0(1)	100.0(1)	100.0(2)	100.0(1)
Radiation	Cu Kα	Cu Kα	Cu Kα	Mo Kα
Crystal system	triclinic	monoclinic	monoclinic	orthorhombic
Space group	$P\bar{1}$	$P2_1/c$	$I2/a$	$Pbca$
a [Å]	7.74992(15)	9.0213(2)	14.22709(18)	11.8738(4)
b [Å]	10.6301(2)	15.6580(3)	15.98244(15)	13.8926(4)
c [Å]	17.3419(4)	26.8420(4)	23.7578(2)	23.7305(8)
α [°]	95.5219(16)	90	90	90
β [°]	95.4644(16)	92.696(2)	100.0828(11)	90
γ [°]	94.6077(16)	90	90	90
Volume [Å^3]	1409.79(5)	3787.38(12)	5318.70(10)	3914.5(2)
Z	2	4	16	8
ρ_{calc} [g cm^{-3}]	1.127	1.744	1.075	1.090
μ [mm^{-1}]	0.473	1.535	0.447	0.061
$F(000)$ [e]	521.314	1968	1888	1408
2Θ range [°]	5.14 – 152.18	6.538 – 151.662	6.698 – 153.158	3.432 – 64.546
Index ranges	$-9 \le h \le 9$ $-13 \le k \le 13$ $-21 \le l \le 20$	$-10 \le h \le 11$ $-19 \le k \le 19$ $-33 \le l \le 33$	$-16 \le h \le 17$ $-20 \le k \le 20$ $-29 \le l \le 29$	$-17 \le h \le 17$ $-20 \le k \le 19$ $-35 \le l \le 35$
Refl. collected	25460	46095	48401	75830
Independent refl.	5803	7640	5551	6693
R_{int}	0.0173	0.0543	0.0303	0.0504
Refl. with $I > 2\sigma(I)$	5052	6294	5031	5117
Data / restraints / parameters	5803 / 0 / 501	7640 / 0 / 631	5551 / 0 / 465	6693 / 0 / 345
Goodness-of-Fit on F^2	1.060	1.027	1.033	1.038
R_1/wR_2 [$I > 2\sigma(I)$]	0.0301 / 0.0850	0.0390 / 0.0956	0.0362 / 0.0903	0.0521 / 0.1330
R_1/wR_2 (all data)	0.0342 / 0.0869	0.0496 / 0.1022	0.0404 / 0.0942	0.0713 / 0.1443
ρ_{fin} (max/min) [e Å^{-3}]	0.32/-0.19	0.30 / −0.27	0.27 / −0.18	0.32 / −0.21
CCDC	2337396	2337397	2337398	2337399

References

[1] P. Niermeier, S. Blomeyer, Y. K. J. Bejaoui, J. L. Beckmann, B. Neumann, H.-G. Stammler and N. W. Mitzel, *Angew. Chem. Int. Ed.* **2019**, *58*, 1965–1969.

[2] G. E. Herberich, U. Eigendorf and U. Englert, *Chem. Ber.* **1993**, *126*, 1397–1402.

[3] M. Radius and F. Breher, *Chem. Eur. J.* **2018**, *24*, 15744–15749.

[4] W. S. Rees, M. D. Hampton, S. W. Hall and J. L. Mills, *Inorg. Synth.* **1990**, *27*, 339–342.

[5] D. J. Parks, W. E. Piers and G. P. A. Yap, *Organometallics* **1998**, *17*, 5492–5503.

[6] D. J. Parks, R. E. von H. Spence and W. E. Piers, *Angew. Chem.* **1995**, *107*, 895–897.

[7] O. V. Dolomanov, L. J. Bourhis, R. J. Gildea, J. A. K. Howard and H. Puschmann, *J. Appl. Crystallogr.* **2009**, *42*, 339.

[8] G. M. Sheldrick, *Acta Crystallogr. A* **2015**, *71*, 3.

[9] G. M. Sheldrick, *Acta Crystallogr. C* **2015**, *71*, 3.

[10] L. J. Bourhis, O. V. Dolomanov, R. J. Gildea, J. A. K Howard, H. Puschmann, *Acta Crystallogr.* **2015**, *A71*, 59-75.

[11] F. Kleemiss, O. V. Dolomanov, M. Bodensteiner, N. Peyerimhoff, L. Midgley, L. J. Bourhis, A. Genoni, L. A. Malaspina, D. Jayatilaka, J. L. Spencer, F. White, B. Grundkötter-Stock, S. Steinhauer, D. Lentz, H. Puschmann, S. Grabowsky, *Chem. Sci.,* **2021**, *12*, 1675 – 1692.